Office of Civilian Radioactive Waste Management

Tip-Over of 12 PWR and 24-BWR Waste Packages
CAL-UDC-ME-000016
REV 00

April 2001

WM-11
NMSS07

OFFICE OF CIVILIAN RADIOACTIVE WASTE MANAGEMENT
CALCULATION COVER SHEET

1. QA: QA

2. Calculation Title
Tip-Over of 12-PWR and 24-BWR Waste Packages

3. Document Identifier (including Revision Number)
CAL-UDC-ME-000016 REV 00

4. Total Attachments	5. Attachment Numbers - Number of pages in each
14	I-3, II-3, III-10, IV-10, Attachments V through XIV are on one CD (See remarks).

	Print Name	Signature	Date
6. Originator	Valérie de la Brosse	V. de la Brosse	04/16/01
7. Checker	Sreten Mastilovic	S. Mastilovic	04/16/01
8. Lead	Scott M. Bennett	Scott M. Bennett	04/16/01

9. Remarks

Attachments V through XIV are electronic media attachments (compact disc) containing ANSYS V5.4 and LS-DYNA V950.C electronic files. The name, size, date and time of cre^a^tion of each file are listed in Section 8 of this document.

SMB 04/16/01

Revision History

10. Revision No.	11. Description of Revision
00	Initial issue

CONTENTS

FIGURES

Page

TABLES

1. PURPOSE

The objective of this calculation was to determine the structural response of a 12-Pressurized Water Reactor (PWR) spent nuclear fuel and a 24-Boiling Water Reactor (BWR) spent nuclear fuel waste packages subjected to tip-over onto an unyielding surface (see Ref. 14, Section 1.2.2.1.6). The scope of this calculation was limited to reporting the calculation results in terms of maximum stress intensities in the inner and outer shells of the waste packages. The information provided by the sketches (Attachments I and II) is that of the potential design of the types of waste packages considered in this calculation, and all obtained results are valid for these designs only. This calculation is associated with the waste package design and was performed by the Waste Package Design Section in accordance with the *Technical work plan for: Waste Package Design Description for LA* (Ref. 13). AP-3.12Q, *Calculations* (Ref. 17), was used to perform the calculation and develop the document.

2. METHOD

The finite element calculations were performed using the commercially available ANSYS version (V) 5.4 and LS-DYNA V950.C finite element codes. ANSYS V5.4 (Ref. 10) was used for preprocessing, i.e., to create finite element representations (FER) used subsequently in LS-DYNA V950.C (Ref. 11) to obtain solutions. The results of these calculations are provided in terms of stress intensities in the outer shell and inner shell.

With regard to the development of this calculation, the control of the electronic management of data was accomplished in accordance with *the Technical work plan for: Waste Package Design Descriptionfor LA* (Ref. 13) and evaluated in accordance with AP-SV.1Q, *Control of the Electronic Management of Information* (Ref. 18). The evaluation (Addendum B of Ref. 13) determined that current work processes and procedures are adequate for the control of electronic management of data for this activity.

3. ASSUMPTIONS

In the course of developing this document, the following assumptions were made regarding the structural calculations for the waste packages.

3.1 Some of the temperature-dependent material properties were not available for SB-575 N06022 (Alloy 22), SA-240 S31600 (316 nuclear grade [NG] stainless steel [SS]), SA-516 K02700 (A 516 Grade 70 carbon steel [CS]), and SA-240 S30400 (304 SS). Therefore, room-temperature (RT) (20°C) material properties were assumed for all materials used. The impact of using RT material properties was anticipated to be small. The rationale for this assumption was that the mechanical properties of these materials do not change significantly at the temperatures experienced during handling and lifting operations. This assumption was used in Section 5.1.

3.2 Some of the rate-dependent material properties were not available for the materials used. Therefore, the material properties obtained under the static loading conditions were assumed for all materials used. The impact of using material properties obtained under static loading conditions was anticipated to be small. The rationale for this assumption was that the mechanical properties of subject materials do not significantly change at the peak strain rates reached in the course of the tip-over. This assumption was used in Section 5.1.

3.3 The Poisson's ratio of Alloy 22 was not available in literature. Therefore, the Poisson's ratio of Alloy 625 (SB-443 N06625) was assumed for Alloy 22. The impact of this assumption was anticipated to be negligible. The rationale for this assumption was that the chemical compositions of Alloy 22 and Alloy 625 are similar (see Ref. 5 and Ref. 2, respectively). This assumption was used in Section 5.1.

3.4 The Poisson's ratio was not available for A 516 Grade 70 CS. Therefore, Poisson's ratio of cast CS was assumed for A 516 Grade 70 CS. The impact of this assumption was anticipated to be negligible. The rationale for this assumption was that the elastic constants of cast CS are only slightly affected by changes in composition and structure (Ref. 4). This assumption was used in Section 5.1.

3.5 The uniform strain of Alloy 22 is not available in the literature. Therefore it is conservatively assumed that the uniform strain is 90% of the elongation. The rationale for this assumption is the character of the stress-strain curve for Alloy 22 (see Ref. 12). This assumption is used in Section 5.1.1.

3.6 The uniform strain of 316NG SS is not available in the literature. Therefore it is conservatively assumed that the uniform strain is 90% of the elongation. The rationale for this assumption is the character of the stress-strain curve for 316 SS (see Ref. 8). This assumption is used in Section 5.1.1.

3.7 The uniform strain of 304 SS is not available in the literature. Therefore it is conservatively assumed that the uniform strain is 75% of the elongation. The rationale for this assumption is the character of the stress-strain curve for 304 SS (see Ref. 8). This assumption is used in Section 5.1.1.

3.8 The uniform strain of A 516 Grade 70 CS is not available in the literature. Therefore it is conservatively assumed that the uniform strain is 50% of the elongation. The rationale for this assumption is the character of the stress-strain curve for A 36 CS (see Ref. 8 and 7) that has similar chemical composition to A 516 Grade 70 CS (see Ref. 5, SA-516/SA-516M and SA-36/SA-36M for chemical compositions of A 516 Grade 70 CS and A 36 CS, respectively). This assumption is used in Section 5.1.1.

3.9 The change of minimum elongation with increase of temperature for the materials used in this calculation is not available in literature. Therefore, the magnitude of this change at T = 316 °C for Alloy 22 and 316NG SS is assumed to be +10% and –30% respectively, based on the relative change of typical elongation for said materials available in vendor catalogues (see Ref. 16 and 1). The rationale for this conservative assumption is that the relative change of typical elongation should be bounding for the relative change of minimum elongation. This assumption is applied just to one calculation for the sake of comparison. This assumption is used in Section 5.1.3.

3.10 The exact geometry of the PWR fuel assembly was simplified for the purpose of this calculation in such a way that its total mass was assumed to be distributed within a bar of square cross section with uniform mass density and constructed of 304 SS. The rationale for this conservative assumption was to provide a set of bounding results, while simplifying the FER. This assumption was used in Section 5.2.1 and 5.5.

3.11 The exact geometry of the BWR fuel assembly was simplified for the purpose of this calculation in such a way that its total mass was assumed to be distributed within a bar of square cross section with uniform mass density and constructed of 304 SS. The rationale for this conservative assumption was to provide a set of bounding results, while simplifying the FER. This assumption was used in Section 5.3.1 and 5.5.

3.12 The mass of the BWR and PWR fuel assemblies were increased by 25 lbs. The rationale for this assumption was to take into account potential variations in the fuel assemblies weight while providing a set of bounding results. This assumption was used in Section 5.2 and 5.3.

3.13 The target surface was conservatively assumed to be unyielding with a large elastic modulus compared to the waste package materials. The rationale for this assumption was that a bounding set of results was required in terms of stresses, and it was known that the use of an unyielding surface with high stiffness ensures slightly higher stresses in the waste package. This assumption was used in Section 5.5.

4. USE OF COMPUTER SOFTWARE AND MODELS

4.1 SOFTWARE

One of the finite element analysis (FEA) computer codes used for this calculation is ANSYS V5.4 (see Ref. 10), which was obtained from Software Configuration Management in accordance with appropriate procedures, and is identified by the Computer Software Configuration Identification number 30040 V5.4. ANSYS V5.4 is a commercially available FEA code and is appropriate for structural calculations of waste packages as performed in this calculation. The calculation using the ANSYS V5.4 software was executed on the Hewlett-Packard (HP) 9000 series workstation identified with YMP (Yucca Mountain Project) tag number 117162. The software qualification of ANSYS V5.4 was summarized in reference 10. The ANSYS evaluation performed for this calculation is fully within the range of the validation performed for the ANSYS V5.4 code. Access to the code was granted by the Software Configuration Secretariat in accordance with the appropriate procedures.

The input files (identified by .inp file extensions) and output files (identified by .out file extensions) for ANSYS V5.4 are provided in Attachments V, VI, X and XI.

The second FEA computer code used for this calculation is Livermore Software Technology Corporation LS-DYNA V950.C (see Ref. 11), which was obtained from the Software Configuration Secretariat in accordance with appropriate procedures, and is identified by the Software Tracking Number 10300-950-00. LS-DYNA V950.C is a commercially available finite element code and is appropriate for structural calculations of waste packages as performed in this calculation. The calculations using LS-DYNA were executed on the HP 9000 series workstation identified with YMP tag number 117162. The LS-DYNA evaluation performed for this calculation is fully within the range of the validation performed for the LS-DYNA V950.C code. Access to the code was granted by the Software Configuration Secretariat in accordance with the appropriate procedures.

The input files (identified by .k and .inc file extensions) and output files (d3hsp) for LS-DYNA V950.C are provided in Attachments V to XIV.

4.2 SOFTWARE ROUTINES

None used.

4.3 MODELS

None used.

5. CALCULATION

5.1 MATERIAL PROPERTIES

Material properties used in these calculations are listed in this section. Some of the temperature-dependent and rate-dependent material properties are not available for Alloy 22, 316NG SS, A 516 Grade 70 CS and 304 SS. Therefore, RT density and RT Poisson's ratio obtained under the static loading conditions are used for for Alloy 22, 316NG SS, A 516 Grade 70 CS and 304 SS (see Assumption 3.1 and 3.2).

SB-575 N06022 (Alloy 22) (outer shell, outer shell lids, extended outer shell lid base, upper and lower trunnion collar sleeves, and inner shell support ring):

- Density = 8690 kg/m^3 (0.314 lb/in^3) (at RT) (Ref. 5, SB-575 Section 7.1)
- Yield strength = 310 *MPa* (45 *ksi*) (at RT) (Ref. 5, Table Y-1)
  Yield strength = 236 *MPa* (34.3 *ksi*) (at 400°*F* = 204°*C*) (Ref. 5, Table Y-1)
  Yield strength = 211 *MPa* (30.6 *ksi*) (at 600°*F* = 316°*C*) (Ref. 5, Table Y-1)
- Tensile strength = 689 *MPa* (100 *ksi*) (at RT) (Ref. 5, Table U)
  Tensile strength = 657 *MPa* (95.3 *ksi*) (at 400°*F* = 204°*C*) (Ref. 5, Table U)
  Tensile strength = 628 *MPa* (91.1 *ksi*) (at 600°*F* = 316°*C*) (Ref. 5, Table U)
- Elongation = 0.45 (at RT) (Ref. 5, SB-575 Table 3)
- Poisson's ratio = 0.278 (at RT) (Ref. 2, p. 143; see Assumption 3.3)
- Modulus of elasticity = 206 *GPa* (at RT) (Ref. 16, p. 14)
  Modulus of elasticity = 196 *GPa* (at 400°*F* = 204°*C*) (Ref. 16, p. 14)
  Modulus of elasticity = 190 *GPa* (at 600°*F* = 316°*C*) (Ref. 16, p. 14)

SA-240 S31600 (316NG SS, which is 316 SS with tightened control on carbon and nitrogen content and has the same material properties as 316 SS [see Ref. 2, page 931 and Ref. 5, Section II, SA-240 Table 1]) (Inner shell and inner shell lids):

- Density = 7980 kg/m^3 (at RT) (Ref. 6, Table X1, p. 7)
- Yield strength = 207 *MPa* (30 *ksi*) (at RT) (Ref. 5, Table Y-1)
  Yield strength = 148 *MPa* (21.4 *ksi*) (at 400°*F* = 204°*C*) (Ref. 5, Table Y-1)
  Yield strength = 130 *MPa* (18.9 *ksi*) (at 600°*F* = 316°*C*) (Ref. 5, Table Y-1)
- Tensile strength = 517 *MPa* (75 *ksi*) (at RT) (Ref. 5, Table U)
  Tensile strength = 496 *MPa* (71.9 *ksi*) (at 400°*F* = 204°*C*) (Ref. 5, Table U)
  Tensile strength = 495 *MPa* (71.8 *ksi*) (at 600°*F* = 316°*C*) (Ref. 5, Table U)

- Elongation = 0.40 (at RT) (Ref. 5, SA-240 Table 2)

- Poisson's ratio = 0.298 (at RT) (Ref. 2, Figure 15, p. 755)

- Modulus of elasticity = 195 GPa ($28.3 \cdot 10^6$ psi) (at RT) (Ref. 5, Table TM-1)
  Modulus of elasticity = 183 GPa ($26.5 \cdot 10^6$ psi) (at 400°F = 204°C) (Ref. 5, Table TM-1)
  Modulus of elasticity = 174 GPa ($25.3 \cdot 10^6$ psi) (at 600°F = 316°C) (Ref. 5, Table TM-1)

SA-516 K02700 (A 516 Grade 70 CS) (basket guides, stiffeners and tubes):

- Density = 7850 kg/m^3 (at RT) (Ref. 5, SA-20/SA-20M, Section 14.1) (Material supplied to ASTM [American Society for Testing and Materials] A 516/A 516M-90 specification shall conform to specification ASTM A 20/A 20M [see Ref. 5, SA-516/SA-516M, section 3.1])

- Yield strength = 262 MPa (38 ksi) (at RT) (Ref. 5, Table Y-1)
  Yield strength = 224 MPa (32.5 ksi) (at 400°F = 204°C) (Ref. 5, Table Y-1)
  Yield strength = 201 MPa (29.1 ksi) (at 600°F = 316°C) (Ref. 5, Table Y-1)

- Tensile strength = 483 MPa (70 ksi) (at RT) (Ref. 5, Table U)
  Tensile strength = 483 MPa (70 ksi) (at 400°F = 204°C) (Ref. 5, Table U)
  Tensile strength = 483 MPa (70 ksi) (at 600°F = 316°C) (Ref. 5, Table U)

- Elongation = 0.21 (at RT) (Ref. 5, SA-516/SA-516M, Table 2)

- Poisson's ratio = 0.3 (at RT) (Ref. 4, p. 374; see Assumption 3.4)

- Modulus of elasticity = 203 GPa ($29.5 \cdot 10^6$ psi) (at RT) (Ref. 5, Table TM-1)
  Modulus of elasticity = 191 GPa ($27.7 \cdot 10^6$ psi) (at 400°F = 204°C) (Ref. 5, Table TM-1)
  Modulus of elasticity = 184 GPa ($26.7 \cdot 10^6$ psi) (at 600°F = 316°C) (Ref. 5, Table TM-1)

SA-240 S30400 (304 SS) (PWR and BWR fuel assemblies):

- Yield strength = 207 MPa (30 ksi) (at RT) (Ref. 5, Table Y-1)
  Yield strength = 143 MPa (20.7 ksi) (at 400°F = 204°C) (Ref. 5, Table Y-1)
  Yield strength = 127 MPa (18.4 ksi) (at 600°F = 316°C) (Ref. 5, Table Y-1)

- Tensile strength = 517 MPa (75 ksi) (at RT) (Ref. 5, Table U)
  Tensile strength = 441 MPa (64 ksi) (at 400°F = 204°C) (Ref. 5, Table U)
  Tensile strength = 437 MPa (63.4 ksi) (at 600°F = 316°C) (Ref. 5, Table U)

- Elongation = 0.40 (at RT) (Ref. 5, SA-240 Table 2)

- Poisson's ratio = 0.29 (at RT) (Ref. 2, Figure 15, p. 755)

- Modulus of elasticity = 195 GPa ($28.3 \cdot 10^6$ psi) (at RT) (Ref. 5, Table TM-1)
  Modulus of elasticity = 183 GPa ($26.5 \cdot 10^6$ psi) (at $400°F = 204°C$) (Ref. 5, Table TM-1)
  Modulus of elasticity = 174 GPa ($25.3 \cdot 10^6$ psi) (at $600°F = 316°C$) (Ref. 5, Table TM-1)

5.1.1 Calculations for True Measures of Ductility

The material properties in Section 5.1 refer to engineering stress and strain definitions: $s = P/A_0$ and $e = L/L_0 - 1$, where P stands for the force applied during static tensile test, L is the deformed-specimen length, and L_0 and A_0 are original length and cross-sectional area of specimen, respectively. The engineering stress-strain curve does not give a true indication of the deformation characteristics of a material during plastic deformation since it is based entirely on the original dimensions of the specimen. In addition, ductile metal that is pulled in tension becomes unstable and necks down during the test. Hence, LS-DYNA V950.C FEA code requires input in terms of true stress and strain definition: $\sigma = P/A$ and $\varepsilon = \ln (L/L_0)$.

The relationships between the true stress and strain definitions and engineering stress and strain definitions, $\sigma = s\,(1+e)$ and $\varepsilon = \ln (1+e)$, can be readily derived based on constancy of volume ($A_0 \cdot L_0 = A \cdot L$) and strain homogeneity during plastic deformation. These expressions are applicable only in the hardening region of stress-strain curve that is limited by the onset of necking.

The following parameters are used in the subsequent calculations:

$s_y \approx \sigma_y$ = yield strength
s_u = engineering tensile strength
σ_u = true tensile strength
$e_y \approx \varepsilon_y$ = strain corresponding to yield strength ($= \frac{\sigma_y}{E}$)
E = modulus of elasticity
e_u = engineering strain corresponding to tensile strength (engineering uniform strain)
ε_u = true strain corresponding to tensile strength (true uniform strain)

In the absence of the uniform strain data in available literature, it needs to be estimated based on the character of stress-strain curves and elongation (strain corresponding to rupture of the tensile specimen).

The stress-strain curves for Alloy 22 and 316NG SS do not manifest three-stage deformation character (see Ref. 12). Therefore, the elongation, reduced by 10% to take into account the specimen-failure part of the stress-strain curve (see Assumptions 3.5 and 3.6), can be used in place of uniform strain for these two materials.

In the case of Alloy 22, ($e_u = 0.9 \cdot \text{elongation} = 0.9 \cdot 0.45 = 0.41$) and the true uniform strain is

$$\varepsilon_u = \ln(1 + e_u) = \ln(1 + 0.41) = 0.34$$

The true tensile strength depends on temperature, thus

$$\sigma_u = s_u \cdot (1 + e_u) = 689 \cdot (1 + 0.41) = 971\, MPa \text{ (at RT)}$$
$$\sigma_u = s_u \cdot (1 + e_u) = 657 \cdot (1 + 0.41) = 926\, MPa \text{ (at } 400°F = 204°C\text{)}$$
$$\sigma_u = s_u \cdot (1 + e_u) = 628 \cdot (1 + 0.41) = 885\, MPa \text{ (at } 600°F = 316°C\text{)}$$

For 316NG SS:

$$e_u = 0.9 \cdot \text{elongation} = 0.9 \cdot 0.40 = 0.36$$
$$\varepsilon_u = \ln(1 + e_u) = \ln(1 + 0.36) = 0.31$$

The true tensile strength on three different temperatures is

$$\sigma_u = s_u \cdot (1 + e_u) = 517 \cdot (1 + 0.36) = 703\, MPa \text{ (at RT)}$$
$$\sigma_u = s_u \cdot (1 + e_u) = 496 \cdot (1 + 0.36) = 675\, MPa \text{ (at } 400°F = 204°C\text{)}$$
$$\sigma_u = s_u \cdot (1 + e_u) = 495 \cdot (1 + 0.36) = 673\, MPa \text{ (at } 600°F = 316°C\text{)}$$

Contrary to the two previous cases, the stress-strain curve for 304 SS exhibits pronounced three-stage (elastic-hardening-softening) deformation character. The uniform strain is, therefore, estimated to be 75% of elongation based on the available stress-strain curves (see Assumption 3.7).

Hence $e_u = 0.75 \cdot \text{elongation} = 0.75 \cdot 0.40 = 0.30$. The true uniform strain is therefore

$$\varepsilon_u = \ln(1 + e_u) = \ln(1 + 0.30) = 0.26$$

The true tensile strength is

$$\sigma_u = s_u \cdot (1 + e_u) = 517 \cdot (1 + 0.30) = 672\, MPa \text{ (at RT)}$$
$$\sigma_u = s_u \cdot (1 + e_u) = 441 \cdot (1 + 0.30) = 573\, MPa \text{ (at } 400°F = 204°C\text{)}$$
$$\sigma_u = s_u \cdot (1 + e_u) = 437 \cdot (1 + 0.30) = 568\, MPa \text{ (at } 600°F = 316°C\text{)}$$

Finally, the stress-strain curve for A 516 Grade 70 CS exhibits stress-strain curve character typical for CS. The uniform strain is estimated to be 50 % of elongation based on the available stress-strain curves for A 36 CS (see Assumption 3.8).

Hence $e_u = 0.5 \cdot \text{elongation} = 0.5 \cdot 0.21 = 0.11$. The true uniform strain is therefore

$\varepsilon_u = \ln(1 + e_u) = \ln(1 + 0.11) = 0.10$

Since the engineering tensile strength of A 516 Grade 70 CS does not vary with temperature for the temperature range of interest, the true tensile strength is

$\sigma_u = s_u \cdot (1 + e_u) = 483 \cdot (1 + 0.11) = 536 MPa$ (at RT, at $400°F = 204°C$, and at $600°F = 316°C$)

5.1.2 Calculations for Tangent Moduli

As previously discussed, the results of this simulation are required to include elastic and plastic deformations for Alloy 22, 316NG SS, A 516 Grade 70 CS and 304 SS. When the materials are driven into the plastic range, the slope of stress-strain curve continuously changes. A ductile failure is preceded by a protracted regime of hardening (and possibly softening) and substantial accumulation of inelastic strains. Thus, a simplification for this curve was needed to incorporate plasticity into the FER. A standard approximation commonly used in engineering is to use a straight line that connects the yield point and the ultimate tensile strength point of the material. The tangent modulus (E_1) is a parameter used in the subsequent calculations in addition to those defined in Section 5.1. The tangent (hardening) modulus represents the slope of the stress-strain curve in the plastic region, and it can be calculated using the following expression: $E_1 = (\sigma_u - \sigma_y)/(\varepsilon_u - \varepsilon_y)$. The tangent moduli are calculated using the preceding expression and material properties given in Sections 5.1 and 5.1.1, and are presented in Table 1.

Table 1. Tangent Moduli at Three Different Temperatures

Material	Tangent Modulus (*GPa*)		
	RT	204 °C	316 °C
Alloy 22	1.95	2.04	1.99
316 NG SS	1.61	1.70	1.76
A 516 CS	2.78	3.16	3.39
304 SS	1.80	1.66	1.70

5.1.3 Effect of Change of Elongation at T = 316 °*C* on Material Properties

The change of minimum elongation with increase of temperature for the materials used in this calculation is not available in literature. Therefore, for Alloy 22 and 316NG SS the magnitude of this change at T = 316 °C is estimated based on the relative change of typical elongation for said materials (see Assumption 3.9). Consequently, the true measures of ductility and tangent moduli, calculated in Sections 5.1.1 and 5.1.2 have to change to accommodate the variability of elongation due to change of temperature.

In case of Alloy 22,

$e_u = 1.1 \cdot (0.9 \cdot \text{elongation}) = 1.1 \cdot (0.9 \cdot 0.45) = 0.45,$

the true uniform strain is therefore

$\varepsilon_u = \ln(1+e_u) = \ln(1+0.45) = 0.37$,

while the true tensile strength is

$\sigma_u = s_u \cdot (1+e_u) = 628 \cdot (1+0.45) = 911\,MPa$ (at $600°F = 316°C$)

Consequently, the tangent modulus becomes

$E_t = (\sigma_u - \sigma_y)/(\varepsilon_u - \sigma_y/E) = (0.911 - 0.211) / (0.37 - 211 / 190 \cdot 10^3) = 1.90\ GPa$

For 316NG SS,

$e_u = 0.7 \cdot (0.9 \cdot \text{elongation}) = 0.7 \cdot (0.9 \cdot 0.40) = 0.25$,

the true uniform strain is therefore

$\varepsilon_u = \ln(1+e_u) = \ln(1+0.25) = 0.22$,

while the true tensile strength is

$\sigma_u = s_u \cdot (1+e_u) = 495 \cdot (1+0.25) = 619\ MPa$ (at $600°F = 316°C$)

Consequently, the tangent modulus becomes

$E_t = (\sigma_u - \sigma_y)/(\varepsilon_u - \sigma_y/E) = (0.619 - 0.130) / (0.22 - 130 / 174 \cdot 10^3) = 2.23\ GPa$

The effects of the change of elongation due to the increase of temperature are taken into account only in one calculation for the sake of comparison with results of the same calculation performed with RT elongation.

5.2 MASS AND GEOMETRIC DIMENSIONS OF PWR FUEL ASSEMBLIES

This calculation was performed by using the following mass and geometric dimensions of the PWR fuel assemblies (Ref. 14, Table I-2, p. 10 and Assumption 3.12):

Total mass = 1920 + 25 = 1945 *lbs* (882.2 *kg*)
Width = 8.4 *in* (213.4 *mm*)
Overall length = 201.1 *in* (5108 *mm*)

5.2.1 Calculation of Density of PWR Fuel Assemblies

This calculation was performed by using the following density for the PWR fuel assemblies (see Assumption 3.10):

$$\text{Density} = \frac{\text{mass}}{\text{volume}} = \frac{\text{mass}}{\text{width}^2 \cdot \text{length}} = \frac{882.2}{0.2134^2 \cdot 5.108} = 3790\,\frac{kg}{m^3}$$

5.3 MASS AND GEOMETRIC DIMENSIONS OF BWR FUEL ASSEMBLIES

This calculation was performed by using the following mass and geometric dimensions of the BWR fuel assemblies (Ref. 14, Table I-1, p. 10 and Assumption 3.12):

Total mass = 669 + 25 = 724 *lbs* (328.4 *kg*)
Width = 5.61 *in* (142.5 *mm*)
Overall length = 173 *in* (4394 *mm*)

5.3.1 Calculation of Density of BWR Fuel Assemblies

This calculation was performed using the following density for the BWR fuel assemblies (see Assumption 3.11):

$$\text{Density} = \frac{\text{mass}}{\text{volume}} = \frac{\text{mass}}{\text{width}^2 \cdot \text{length}} = \frac{328.4}{0.1425^2 \cdot 4.394} = 3680\,\frac{kg}{m^3}$$

5.4 INITIAL VELOCITY OF WASTE PACKAGE

To reduce the computer execution time while preserving all features of the problem relevant to the structural calculation, the waste package is set in a position just before impact and given an appropriate initial rotational velocity.

The following parameters are used in the subsequent paragraph :

w = rotational velocity
m = total mass
g = acceleration due to gravity
h = distance of the center of gravity (CG) from the unyielding surface
I = mass moment of inertia around x axis
PE = potential energy = m·g·h
KE = kinetic energy = $I \cdot w^2/2$

Using the principle of conservation of energy between two positions 0 and 1,

$$PE_0 + KE_0 = PE_1 + KE_1$$

Position 0 is chosen when the waste package reaches the angle necessary for tip-over (see Figure 1). The angle is then γ_0=arctg (L/[D/2]). Position 1 is chosen when the waste package is about to reach the unyielding surface; the angle is then γ_1=0.1°.

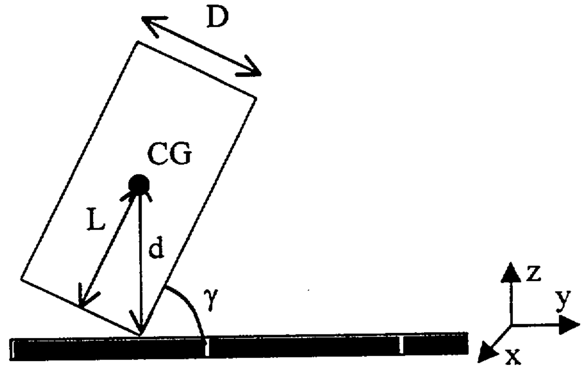

Figure 1. Tip-over Geometry

The following parameters are introduced in Figure 1:

L = distance in the axial direction to the CG from the base of the waste package
D = outside diameter of the trunnion collar sleeve
d = distance between the CG and the center of rotation

At t = t_0, the rotational velocity is considered to be zero, so $KE_0 = 0$. The potential energy is $PE_0 = m \cdot g \cdot h_0$.

At t = t_1, the potential energy of the waste package is $PE_1 = m \cdot g \cdot h_1$, and the kinetic energy is $KE_1 = I \cdot w_1^2/2$.

So $m \cdot g \cdot h_0 - m \cdot g \cdot h_1 = I \cdot w_1^2/2$ and

$$w_1 = \sqrt{\frac{2\, m \cdot g \cdot (h_0 - h_1)}{I}} \quad (1)$$

where

$$h_i = \frac{D}{2} \cdot \cos\gamma_i + L \cdot \sin\gamma_i, \quad i = 0, 1 \quad (2)$$

The mass moment of inertia about the x axis located at the center of gravity (Ix) was calculated using LS-DYNA V950.C with the unyielding surface omitted (see Attachments V and X).

Using the parallel axis thereom, the mass moment of inertia about the center of rotation is

$$I = Ix + m \cdot d^2 \quad (3)$$

where

$$d = \sqrt{L^2 + \left(\frac{D}{2}\right)^2} \quad (4)$$

For the 12-PWR waste package, the following results block was taken from Attachment V, d3hsp, lines 199865 through 199881:

```
m a s s   p r o p e r t i e s   o f   b o d y
   total mass of body          =   .3014E+05
   x-coordinate of mass center =  -.1386E-06
   y-coordinate of mass center =   .6689E+00
   z-coordinate of mass center =   .2845E+01

   inertia tensor of body
   row1=   .8454E+05    .1667E-02    .1432E-02
   row2=   .1667E-02    .8433E+05   -.8406E+01
   row3=   .1432E-02   -.8406E+01    .6813E+04

   principal inertias of body
   i11 =   .8454E+05
   i22 =   .8433E+05
   i33 =   .6813E+04
```

Note that the mass calculated from LS-DYNA V950.C is slightly higher than that listed in Attachment I, due to the 4-*mm* radial gap between the inner and outer shells, as opposed to the 0-*mm* radial gap in Attachment I. The impact was anticipated to be negligible; however, the mass listed above was used in the subsequent calculations as the bounding mass.

The parameter L corresponds to the z-coordinate of the center of mass obtained from LS-DYNA V950.C output file d3hsp.

In this case, the waste package is rotating about the x axis, thus $Ix = i_{11} = 8.454 \cdot 10^4$ $kg \cdot m^2$.

For the 24-BWR waste package, the following results block was taken from Attachment X, d3hsp, lines 184695 through 184711:

```
m a s s   p r o p e r t i e s   o f   b o d y
   total mass of body          =   .2872E+05
   x-coordinate of mass center =  -.9668E-07
   y-coordinate of mass center =   .6630E+00
   z-coordinate of mass center =   .2569E+01

   inertia tensor of body
   row1=   .6509E+05   -.9501E-02   -.2021E-01
```

row2= -.9501E-02 .6503E+05 -.8664E+01
row3= -.2021E-01 -.8664E+01 .6477E+04

principal inertias of body
i11 = .6509E+05
i22 = .6503E+05
i33 = .6477E+04

Note that the mass calculated from LS-DYNA V950.C is slightly higher than that listed in Attachment II, due to the 4-*mm* radial gap between the inner and outer shells, as opposed to the 0-*mm* radial gap in Attachment II. The impact was anticipated to be negligible; however, the mass listed above was used in the subsequent calculations as the bounding mass.

In this case, the waste package is rotating about the x axis, thus $Ix = i_{11} = 6.509 \cdot 10^4$ $kg \cdot m^2$.

Table 2. Numerical Values Needed to Calculate the Initial Rotational Velocity of the Waste Packages

	12-PWR	24-BWR
g (*m/s²*)	9.81	
m (*kg*)	30140 Attachment V, d3hsp, line 199866	28720 Attachment X, d3hsp, line 184696
L (*m*)	2.845 Attachment V, d3hsp, line 199869	2.569 Attachment X, d3hsp, line 184699
D (*m*)	1.338 Attachment I, see remark below	1.326 Attachment II, see remark below
Ix (*kg. m²*)	$8.454 \cdot 10^4$ Attachment V, d3hsp, line 199879	$6.509 \cdot 10^4$ Attachment X, d3hsp, line 184709
h_0 (*m*) Eq. (2)	2.92	2.65
h_1 (*m*) Eq. (2)	0.674	0.667
d (*m*) Eq. (4)	2.92	2.65
I (*kg. m²*) Eq. (3)	$3.42 \cdot 10^5$	$2.67 \cdot 10^5$
w (*rad/s*) Eq. (1)	2.0	2.0

Remark: The value of D (outermost diameter of the waste packages) for the 12-PWR and the 24-BWR is larger in the FER than in Attachments I and II, since the FER takes into account a 4-*mm* radial gap between the inner and outer shells that is not represented in the attachments (see Ref. 15).

5.5 FINITE ELEMENT REPRESENTATIONS

A three-dimensional FER of each waste package was developed in ANSYS V5.4 using the dimensions provided in Attachments I and II. The FERs were created with the largest possible radial gap of 4 *mm* between the inner and outer shell (Ref. 15). The initial orientation of the inner shell maintained this 4-*mm* gap around the circumference of the shell. The internal structure of the waste packages was simplified in several ways. First the support tubes, brackets, and divider plates were combined and created as shell elements. Next, the structures of the PWR and BWR fuel assemblies were reduced to bars of square cross section of uniform mass density, and assumed to be constructed of 304 SS (Assumptions 3.10 and 3.11). The total mass and geometric dimensions of the PWR and BWR fuel assemblies (see Sections 5.2 and 5.3) define their respective density. The lid lifting features are not represented in the FER. Nevertheless, their mass is taken into account in the mass of the lid they are attached to. Furthermore, the densities of all other components of the waste packages were adjusted so that the masses of the waste packages match the masses given in Attachments I and II. (The masses of the outer shells were increased to take into account the increase of volume resulting from the 4-mm gap represented in the FER.)

The benefit of using this approach was to reduce the computer execution time while preserving all features of the problem relevant to the structural calculation.

The target surface was conservatively assumed to be unyielding with a large elastic modulus (Assumption 3.13).

The mesh of each FER was appropriately generated and refined in the contact region according to standard engineering practice. Thus, the accuracy and representativeness of the results of this calculation were deemed acceptable. The meshes of the 12-PWR and the 24-BWR waste packages are presented in Figures III-1 and IV-1 respectively.

The initial tip-over angle was reduced to 0.1°, and each waste package was given an initial rotational velocity corresponding to its rigid-body motion (see Section 5.4).

Each FER was then used in LS-DYNA V950.C to perform the transient dynamic analysis for the 12-PWR and 24-BWR waste packages tip-over (See Ref. 14) at RT, 204 $°C$, and 316 $°C$.

6. RESULTS

This document may be affected by technical product input information that requires confirmation. Any changes to the document that may occur as a result of completing the confirmation activities will be reflected in subsequent revisions. The status of the technical product input information quality may be confirmed by review of the DIRS database.

The results obtained from LS-DYNA V950.C were reported in terms of maximum shear stress. Since the maximum stress intensities were desired, the results needed to be converted. The maximum shear stress is defined as one half the difference between maximum and minimum principal stress. Stress intensity is defined as the difference between maximum and minimum principal stress. Therefore, the results obtained from LS-DYNA V950.C were multiplied by two, to obtain the corresponding stress intensities.

The maximum stresses were found by carefully examining each time step taken by LS-DYNA V950.C, which outputs the element with the highest magnitude of stress, at each step, for each defined part. Table 3 lists the maximum stress intensities in the outer shell and inner shell of the 12-PWR waste package at three different temperatures: RT, 204 $°C$, and 316 $°C$.

Table 3. Maximum Stress Intensities for the 12-PWR Waste Package

Temperature	12-PWR	
	Inner Shell	Outer Shell
RT	466 MPa (see Att. III, Figure 2)	626 MPa (see Att. III, Figure 3)
204 °C	429 MPa (see Att. III, Figure 4)	567 MPa (see Att. III, Figure 5)
316 °C	415 MPa (see Att. III, Figure 6)	551 MPa (see Att. III, Figure 7)

The maximum stress intensities in the outer and inner shells of the 24-BWR waste package at three different temperatures: RT, 204 $°C$, and 316 $°C$ are presented in Table 4.

Table 4. Maximum Stress Intensities for the 24-BWR Waste Package

Temperature	24-BWR	
	Inner Shell	Outer Shell
RT	443 MPa (see Att. IV, Figure 2)	635 MPa (see Att. IV, Figure 3)
204 °C	398 MPa (see Att. IV, Figure 4)	553 MPa (see Att. IV, Figure 5)
316 °C	388 MPa (see Att. IV, Figure 6)	523 MPa (see Att. IV, Figure 7)

The same results are presented in Table 5 in non-dimensional form. The Sint/σ_u and Sint/σ_y represent ratios of the stress intensity (Sint) (presented in Tables 3 and 4) and the tensile and yield strength (presented in Sections 5.1.1 and 5.1), respectively, at the temperatures of interest in this calculation.

Table 5. Stress Intensity in Non-dimensional Form in Inner and Outer Shell for three Different Temperatures.

	12-PWR				24-BWR			
	Inner Shell		Outer Shell		Inner Shell		Outer Shell	
Temperature (°C)	Sint/σ_y	Sint/σ_u	Sint/σ_y	Sint/σ_u	Sint/σ_y	Sint/σ_u	Sint/σ_y	Sint/σ_u
20	2.3	0.66	2.0	0.64	2.1	0.30	2.0	0.65
204	2.9	0.64	2.4	0.61	2.7	0.59	2.3	0.60
316	3.2	0.62	2.6	0.62	3.0	0.58	2.5	0.59

The above table shows that for each temperature condition, the maximum stress intensity in the outer shell exceeded the yield strength of Alloy 22, but the magnitude was less than 70% of the tensile strength of this material (see Sections 5.1 and 5.1.1).

In the absence of data in literature, the change of minimum elongation with increase of temperature for Alloy 22 and 316NG SS at T = 316 °*C* is estimated based on the relative change of typical elongation of these materials (Section 5.1.3). This change in input data reflects on the calculation results. Thus, in the case where the temperature-induced variation of the minimum elongation is taken into account, the maximum stress intensities in the inner and outer shell of the 12-PWR waste package are 456 MPa (see Figure III-7) and 544 MPa (see Figure III-8), respectively. In the 24-BWR waste package, they are 426 MPa (inner shell, see Figure IV-7) and 515 MPa (outer shell, see Figure IV-8). These results are presented in Table 6 in non-dimensional form (row "changing" elongation) for comparison with the results obtained previously by assuming that the change of elongation due to temperature for Alloy 22 and 316NG SS is negligible (row "constant" elongation). The values of σ_y are issued from Section 5.1, the values of σ_u from Section 5.1.3.

Table 6. Stress Intensities in Non-dimensional Form in the Waste Packages at 316 °C for Two Different Approaches Concerning Change of Elongation with Temperature

	12-PWR				24-BWR			
	Inner Shell		Outer Shell		Inner Shell		Outer Shell	
Elongation	Sint/σ_y	Sint/σ_u	Sint/σ_y	Sint/σ_u	Sint/σ_y	Sint/σ_u	Sint/σ_y	Sint/σ_u
constant	3.2	0.62	2.6	0.62	3.0	0.58	2.5	0.59
changing	3.5	0.74	2.6	0.60	3.3	0.69	2.4	0.57

This table shows that using a constant elongation gives conservative results in the outer shell. In the inner shell, though, the results are conservative when the change of elongation with temperature is taken into account.

7. REFERENCES

1. Allegheny Ludlum 1999. "Technical Data Blue Sheet, Stainless Steels, Chromium-Nickel-Molybdenum, Types 316 (S31600), 316L (S31603), 317 (S31700), 317L (S31703)." Pittsburgh, Pennsylvania: Allegheny Ludlum Corporation. Accessed July 31, 2000. TIC: 248631. http://www.alleghenytechnologies.com/ludlum/pages/products/t316_317.pdf

2. ASM (American Society for Metals) 1980. *Properties and Selection: Stainless Steels, Tool Materials and Special-Purpose Metals.* Volume 3 of *Metals Handbook.* 9th Edition. Benjamin, D., ed. Metals Park, Ohio: American Society for Metals. TIC: 209801.

3. ASM International 1987. *Corrosion.* Volume 13 of *Metals Handbook.* 9th Edition. Metals Park, Ohio: ASM International. TIC: 209807.

4. ASM International 1990. *Properties and Selection: Irons, Steels, and High-Performance Alloys.* Volume 1 of *Metals Handbook.* 10th Edition. Materials Park, Ohio: ASM International. TIC: 245666.

5. ASME (American Society of Mechanical Engineers) 1998. *1998 ASME Boiler and Pressure Vessel Code.* 1998 Edition, Including Addenda. New York, New York: American Society of Mechanical Engineers. TIC: 247429.

6. ASTM G 1-90 (Reapproved 1999). 1990. *Standard Practice for Preparing, Cleaning, and Evaluating Corrosion Test Specimens.* West Conshohocken, Pennsylvania: American Society for Testing and Materials. TIC: 238771.

7. Bowles, J.E. 1980. *Structural Steel Design*. New York, New York: McGraw-Hill. TIC: 249182.

8. Boyer, H.E., ed. 2000. *Atlas of Stress-Strain Curves.* Metals Park, Ohio: ASM International. TIC: 248901.

9. CRWMS M&O 1997. *Waste Container Cavity Size Determination*. BBAA00000-01717-0200-00026 REV 00. Las Vegas, Nevada: CRWMS M&O. ACC:MOL.19980106.0061

10. CRWMS M&O 1998. *ANSYS.* V5.4. HP-UX 10.20. 30040 5.4.

11. CRWMS M&O 2000. *Software Code: LS-DYNA*. V950. HP 9000. 10300-950-00.

12. CRWMS M&O 2000. *Stress-strain-curve character for Alloy 22 and 316 Stainless Steel.* Input Transmittal 00384.T. Las Vegas, Nevada: CRWMS M&O. ACC: MOL.20001013.0053.

13. CRWMS M&O 2000. *Technical Work Plan for: Waste Package Design Description for LA.* TWP-EBS-MD-000004 REV 00. Las Vegas, Nevada: CRWMS M&O. ACC: MOL.20001107.0304.

14. CRWMS M&O 2000. *Uncanistered Spent Nuclear Fuel Disposal Container System Description Document.* SDD-UDC-SE-000001 REV 01. Las Vegas, Nevada: CRWMS M&O. ACC: MOL.20000822.0004.

15. CRWMS M&O 2000. *Waste Package Operations Fabrication Process Report.* TDR-EBS-ND-000003 REV 01. Las Vegas, Nevada: CRWMS M&O. ACC: MOL.20000927.0002.

16. Haynes International 1997. *Hastelloy C-22 Alloy.* Kokomo, Indiana: Haynes International. TIC: 238121.

17. AP-3.12Q, Rev. 0, ICN 4. *Calculations.* Washington, D.C.: U.S. Department of Energy, Office of Civilian Radioactive Waste Management. ACC: MOL.20010404.0008

18. AP-SV.1Q, Rev. 0, ICN 2. *Control of the Electronic Management of Information.* Washington, D.C.: U.S. Department of Energy, Office of Civilian Radioactive Waste Management. ACC: MOL.20000831.0065

8. ATTACHMENTS

Attachment I: Design sketches (*12-PWR long waste package configuration for Site Recommendation* [SK-0183 REV 01]. This attachment uses Ref. 9)

Attachment II: Design sketches (*24-BWR waste package configuration for Site Recommendation* [SK-0184 REV 00]. This attachment uses Ref. 9)

Attachment III: Figures obtained from LS-DYNA V950.C for the tip-over of the 12-PWR waste package

Attachment IV: Figures obtained from LS-DYNA V950.C for the tip-over of the 24-BWR waste package

Attachments V to IX (Compact Disc):
ANSYS V5.4 and LS-DYNA V950.C electronic files for the tip-over of the 12-PWR waste package (Attachments VII to IX use the same .inc, .inp, and .out files as Attachment VI)

Attachments X to XIV (Compact Disc):
ANSYS V5.4 and LS-DYNA V950.C electronic files for the tip-over of the 24-BWR waste package (Attachments XII to XIV use the same .inc, .inp, and .out files as Attachment XI)

Table 7 contains the name, size, date and time of creation of each file in Attachments V to XIV.

Table 7. Name, Size, Date and Time of Creation of the Files in Attachments V to XIV

Attachment # and title	Name	Size (Kbytes)	Date	Time
V: Determination of the inertia of the 12-PWR waste package	bc12pi.inc	11	3/21/01	2:25 pm
	d3hsp	14,998	3/21/01	2:25 pm
	e12pi.inc	3,509	3/21/01	2:24 pm
	inert12P.k	5	3/21/01	2:24 pm
	INERT12P.inp	30	3/21/01	2:24 pm
	INERT12P.out	744	3/21/01	2:24 pm
	n12pi.inc	3,529	3/21/01	2:24 pm
VI: Room temperature calculation for the 12-PWR waste package	12PWR_RT.k	5	3/21/01	2:26 pm
	bc12.inc	2	3/21/01	2:25 pm
	d3hsp	15,558	3/21/01	2:26 pm
	e12.inc	3,538	3/21/01	2:25 pm
	gape12P.inp	31	3/21/01	2:25 pm
	gape12P.out	754	3/21/01	2:25 pm
	n12.inc	3,565	3/21/01	2:25 pm
VII : Calculation for the 12-PWR waste package at 400° *F*	12PWR_400F.k	5	3/21/01	2:27 pm
	d3hsp	15,545	3/21/01	2:27 pm
VIII: Calculation for the 12-PWR waste package at 600° *F*	12PWR_600F.k	5	3/21/01	2:28 pm
	d3hsp	15,538	3/21/01	2:28 pm
IX: Calculation for the 12-PWR waste package at 600° *F*, with the modified value of elongation	12PWR_600FM.k	5	3/21/01	2:28 pm
	d3hsp	15,538	3/21/01	2:28 pm
X: Determination of the inertia of the 24-BWR waste package	bc24bi.inc	27	3/21/01	2:30 pm
	d3hsp	13,952	3/21/01	2:30 pm
	e24bi.inc	3,128	3/21/01	2:29 pm
	INERT24B.inp	33	3/21/01	2:29 pm
	INERT24B.out	756	3/21/01	2:29 pm
	maininert24B.k	5	3/21/01	2:29 pm
	n24bi.inc	3,208	3/21/01	2:29 pm
XI: Room temperature calculation for the 24-BWR waste package	bc24.inc	2	3/21/01	2:30 pm
	d3hsp	14,421	3/21/01	2:31 pm
	e24.inc	3,155	3/21/01	2:30 pm
	gape24B.inp	34	3/21/01	2:30 pm
	gape24B.out	766	3/21/01	2:30 pm
	24B_RT.k	5	3/21/01	2:31 pm
	n24.inc	3,240	3/21/01	2:30 pm
XII: Calculation for the 24-BWR waste package at 400° *F*	d3hsp	14,408	3/21/01	2:32 pm
	24B_400F.k	5	3/21/01	2:32 pm
XIII: Calculation for the 24-BWR waste package at 600° *F*	d3hsp	14,402	3/21/01	2:33 pm
	24B_600F.k	5	3/21/01	2:33 pm
XIV: Calculation for the 24-BWR waste package at 600° *F*, with the modified value of elongation	d3hsp	14,401	3/21/01	2:33 pm
	24B_600M.k	5	3/21/01	2:33 pm

ATTACHMENT I

Design sketches

(*12-PWR long waste package configuration for site recommendation* [SK-0183 REV 01])

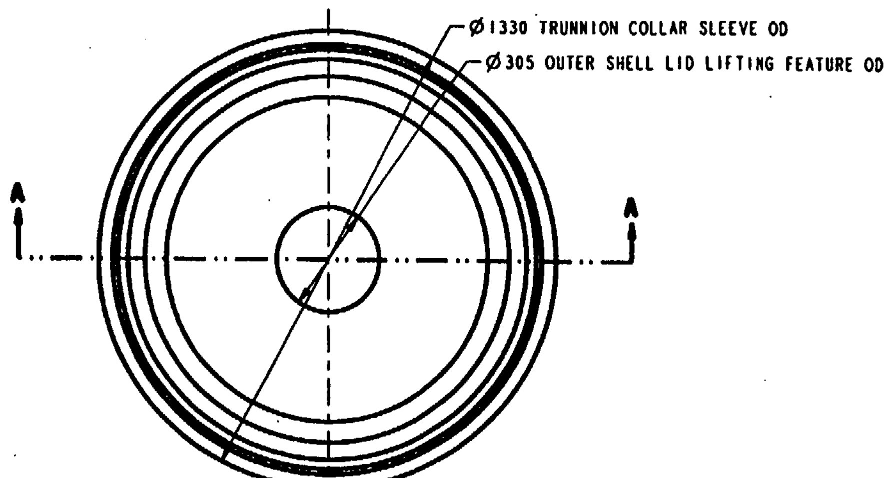

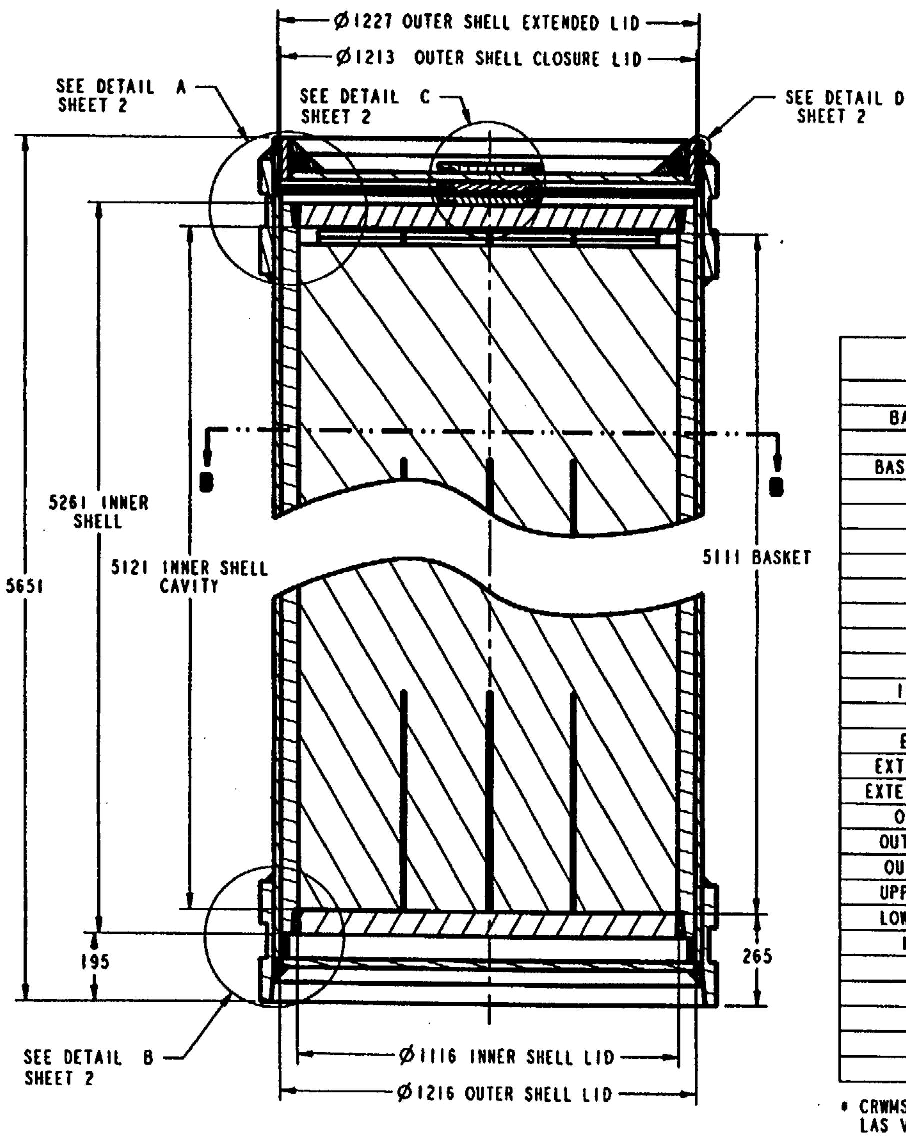

SECTION A-A

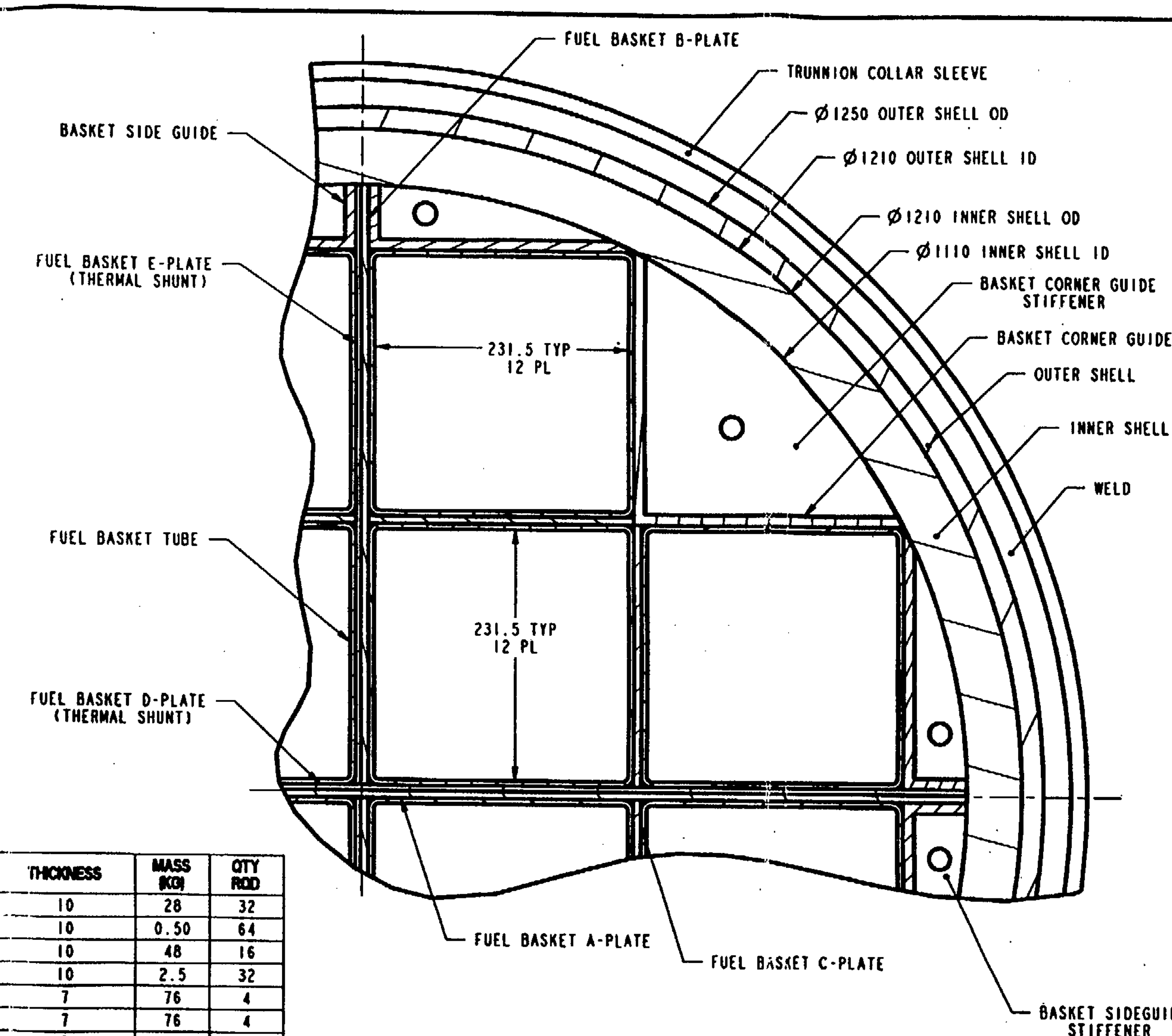

SECTION B-B

COMPONENT NAME	MATERIAL	THICKNESS	MASS (KG)	QTY ROD
BASKET SIDEGUIDE	SA-516 K02700	10	28	32
BASKET SIDEGUIDE STIFFENER	SA-516 K02700	10	0.50	64
BASKET CORNER GUIDE	SA-516 K02700	10	48	16
BASKET CORNER GUIDE STIFFENER	SA-516 K02700	10	2.5	32
FUEL BASKET A-PLATE	NEUTRONIT A 978	7	76	4
FUEL BASKET B-PLATE	NEUTRONIT A 978	7	76	4
FUEL BASKET C-PLATE	NEUTRONIT A 978	7	34	16
FUEL BASKET D-PLATE	SB-209 A96061 T4	5	19	4
FUEL BASKET E-PLATE	SB-209 A96061 T4	5	19	4
FUEL BASKET TUBE	SA-516 K02700	5	187	12
INNER SHELL	SA-240 S31600	50	7589	1
INNER SHELL LID	SA-240 S31600	70	538	2
INNER LID LIFTING FEATURE	SA-240 S31600	27	12	1
OUTER SHELL	SB-575 N06022	(01) 20	3666	1
EXTENDED OUTER SHELL LID	SB-575 N06022	25	104	1
EXTENDED OUTER SHELL LID BASE	SB-575 N06022	25	226	1
EXTENDED LID REINFORCEMENT RING	SB-575 N06022	50	76	1
OUTER LID LIFTING FEATURE	SB-575 N06022	27	13	2
OUTER SHELL FLAT CLOSURE LID	SB-575 N06022	10	100	1
OUTER SHELL FLAT BOTTOM LID	SB-575 N06022	25	250	1
UPPER TRUNNION COLLAR SLEEVE	SB-575 N06022	40	408	1
LOWER TRUNNION COLLAR SLEEVE	SB-575 N06022	40	400	1
INNER SHELL SUPPORT RING	SB-575 N06022	20	32	1
TOTAL ALLOY 22 WELDS	SFA-5.14 N06022	-	196	**
TOTAL 316 WELDS	SFA-5.9 S31680	-	67	**
WASTE PACKAGE ASSEMBLY	-	-	19541	1
PWR FUEL ASSEMBLY	-	-	882.2*	12
WP ASSEMBLY WITH SNF	-	-	30127	1

* CRWMS M&O 1997. WASTE CONTAINER CAVITY SIZE DETERMINATION. BBAA00000-01717-0200-00026 REV 00
LAS VEGAS, NEVADA: CRWMS M&O. ACC: MOL. 19980106-0061

** REFER TO SK-0205 REV 00 "12-PWR LONG PACKAGE WELD CONFIGURATION"

UNITS: mm

DO NOT SCALE FROM SKETCH

(01)

REVISIONS			
REV	DESCRIPTION	DWN BY	DATE
00	ISSUED APPROVED	GC	01/26/00
01	20 OUTER SHELL THICKNESS "WAS" 25. REVISION TABLE "ADDED"	BH	03/23/00

"FOR INFORMATION ONLY"

12-PWR LONG WASTE PACKAGE CONFIGURATION FOR SITE RECOMMENDATION

SKETCH NUMBER: SK-0183 REV 01 — SHEET 1 OF 2

SKETCHED BY: BRYAN HARKINS BH 23 March 00 — Z.C. for SMB 3/23/00

DATE: 03/23/00 — TWD 3.23.00 — [signature] 3/23/00

FILE: /home/pro_library/checkout/sketches/12pwr/12pwr_long/SK-0183.dwg

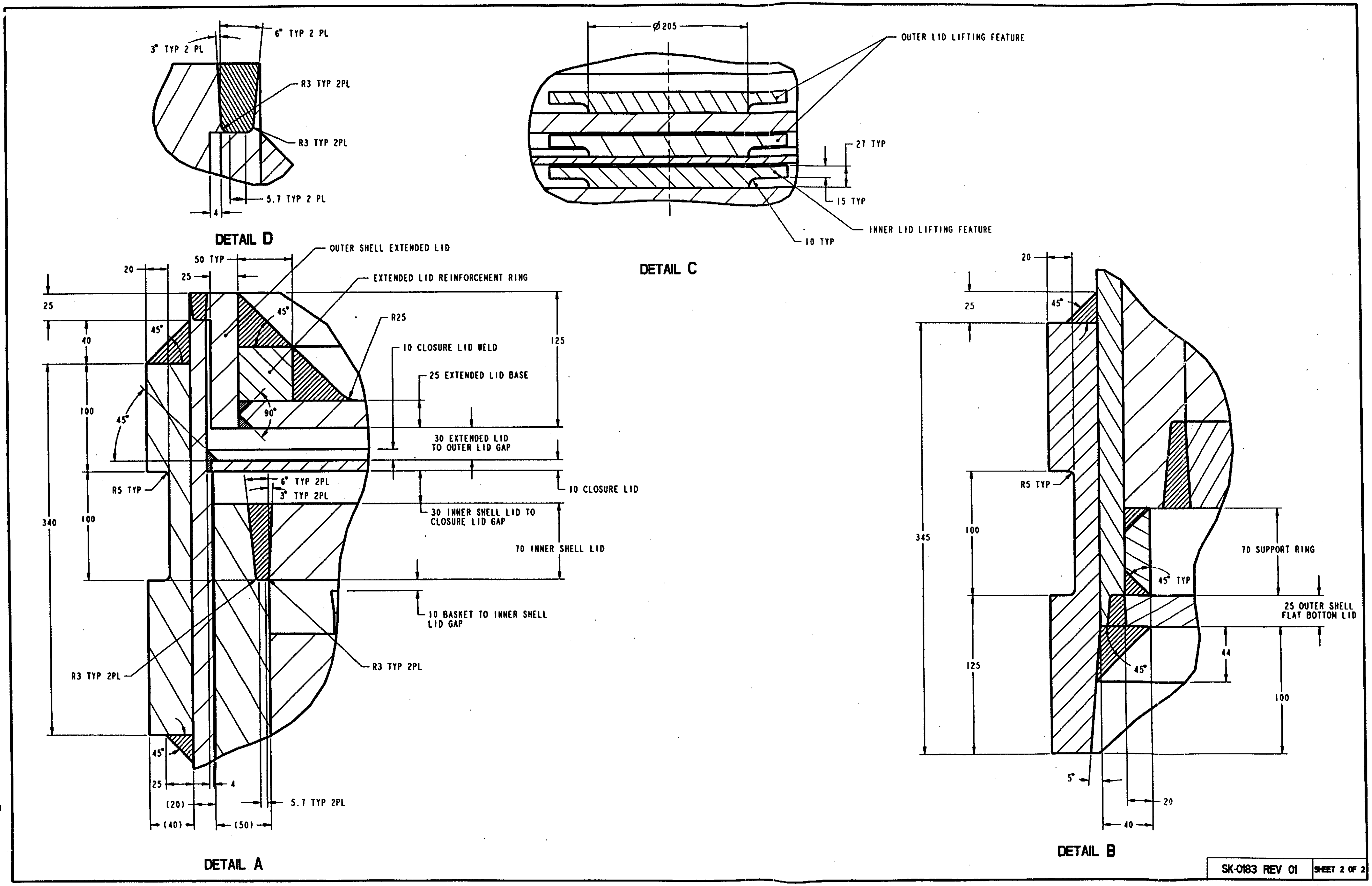

DETAIL D
3° TYP 2 PL
6° TYP 2 PL
R3 TYP 2PL
R3 TYP 2PL
5.7 TYP 2 PL
4
DETAIL C
Ø205
OUTER LID LIFTING FEATURE
27 TYP
15 TYP
INNER LID LIFTING FEATURE
10 TYP
DETAIL A
OUTER SHELL EXTENDED LID
EXTENDED LID REINFORCEMENT RING
R25
10 CLOSURE LID WELD
25 EXTENDED LID BASE
30 EXTENDED LID TO OUTER LID GAP
10 CLOSURE LID
30 INNER SHELL LID TO CLOSURE LID GAP
70 INNER SHELL LID
10 BASKET TO INNER SHELL LID GAP
R3 TYP 2PL
R3 TYP 2PL
R5 TYP
6° TYP 2PL
3° TYP 2PL
50 TYP
20
25
25
40
100
100
340
125
45°
45°
45°
45°
90°
25
(20)
(40)
(50)
4
5.7 TYP 2PL
DETAIL B
20
25
45°
R5 TYP
345
100
125
70 SUPPORT RING
45° TYP
25 OUTER SHELL FLAT BOTTOM LID
44
100
45°
5°
20
40
SK-0183 REV 01
SHEET 2 OF 2

ATTACHMENT II

Design sketches

(*24-BWR waste package configuration for site recommendation* [SK-0184 REV 00])

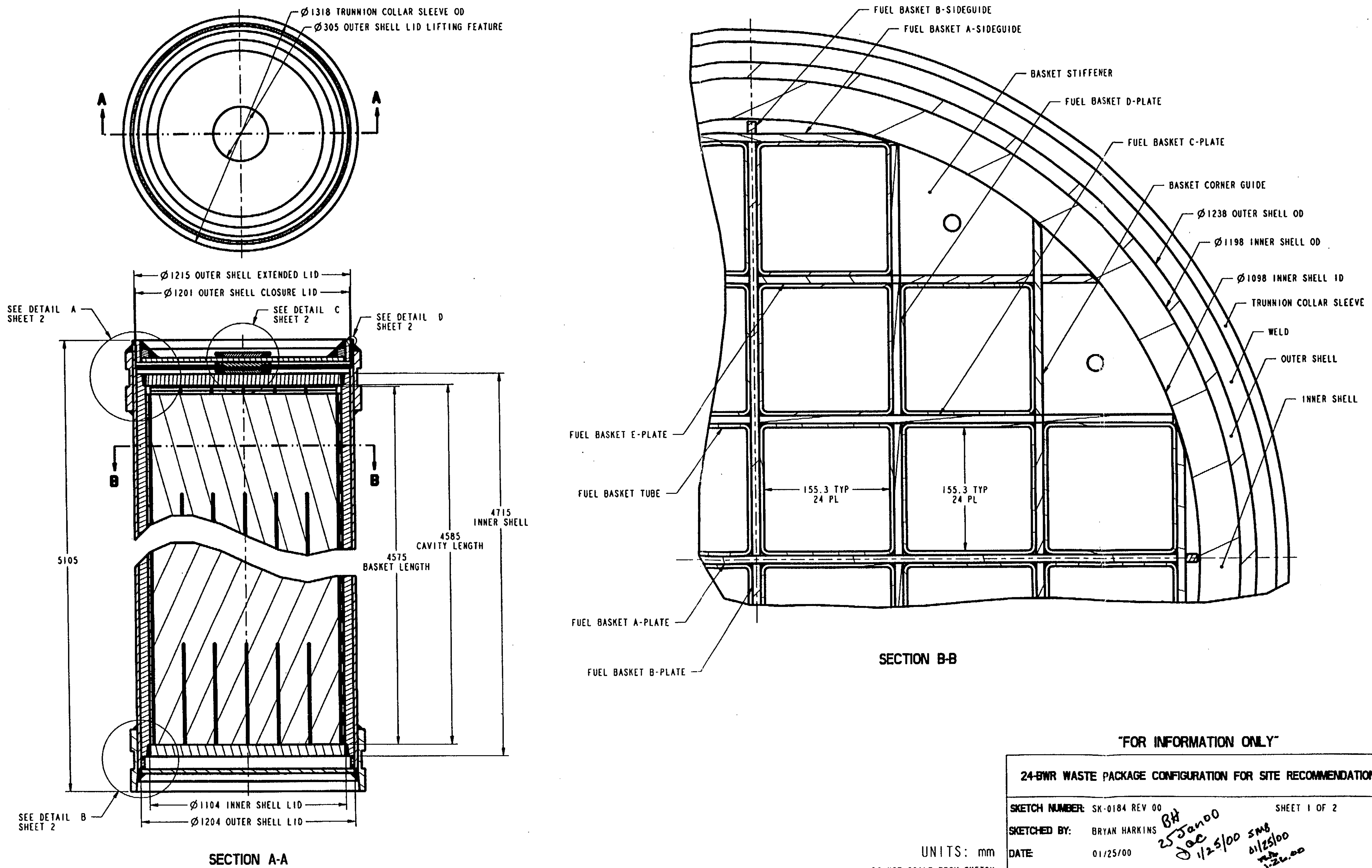

"FOR INFORMATION ONLY"

UNITS: mm

DO NOT SCALE FROM SKETCH

24-BWR WASTE PACKAGE CONFIGURATION FOR SITE RECOMMENDATION		
SKETCH NUMBER:	SK-0184 REV 00	SHEET 1 OF 2
SKETCHED BY:	BRYAN HARKINS	
DATE:	01/25/00	
FILE:	/home/pro_library/checkout/sketches/24-bwr/sk-0184.dwg	

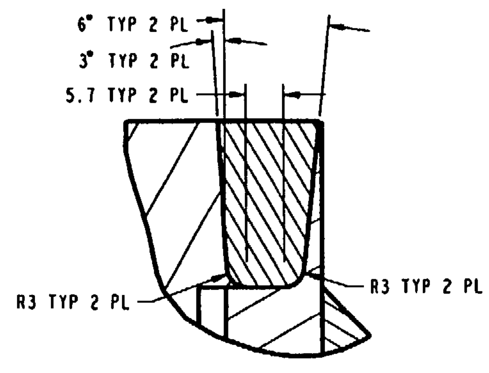

DETAIL D

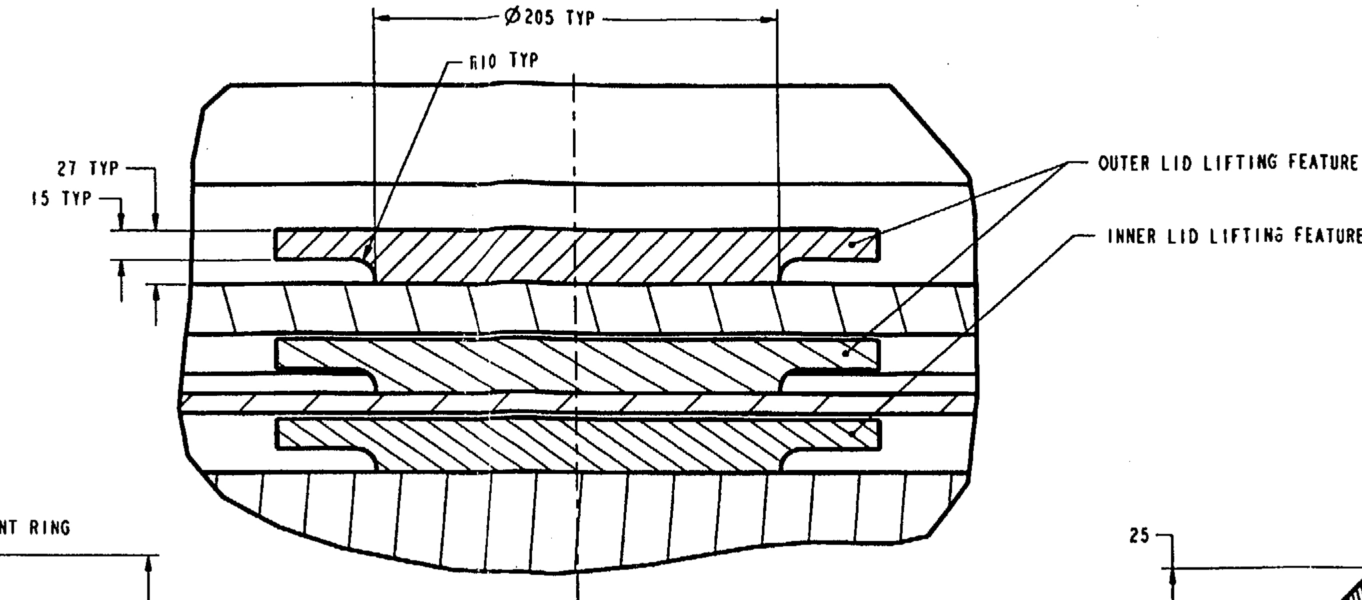

DETAIL C

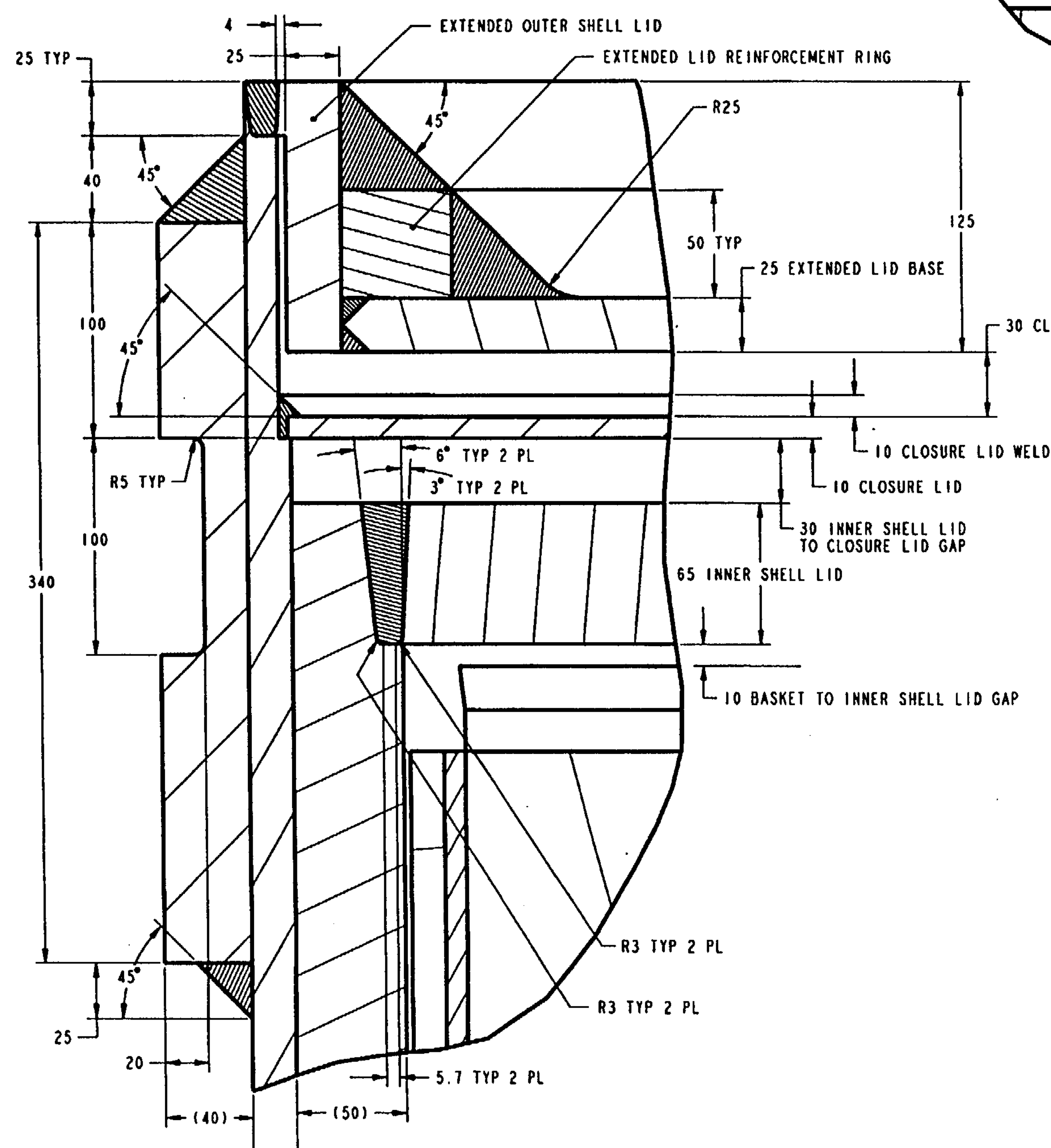

DETAIL A

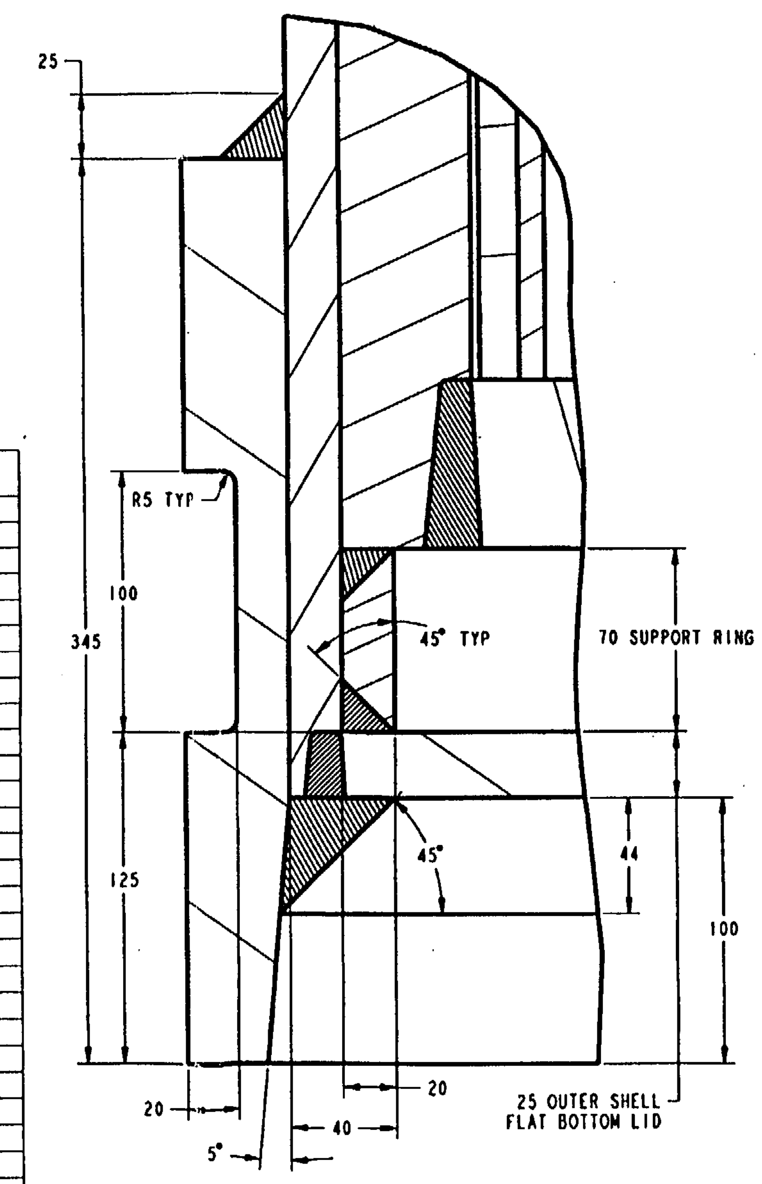

DETAIL B

COMPONENT NAME	MATERIAL	THICKNESS	MASS (KG)	QTY RQD
BASKET A-GUIDE	SA-516 K02700	10	27	16
BASKET B-GUIDE	SA-516 K02700	10	1.3	16
BASKET CORNER GUIDE	SA-516 K02700	10	22	32
BASKET STIFFENER	SA-516 K02700	10	1.6	64
FUEL BASKET A-PLATE	NEUTRONIT A 978	10	89	4
FUEL BASKET B-PLATE	NEUTRONIT A 978	10	89	4
FUEL BASKET C-PLATE	NEUTRONIT A 978	10	90	8
FUEL BASKET D-PLATE	NEUTRONIT A 978	10	90	8
FUEL BASKET E-PLATE	NEUTRONIT A 978	10	30	16
FUEL BASKET TUBE	SA-516 K02700	5	113	24
INNER SHELL	SA-240 S31600	50	6731	1
INNER SHELL LID	SA-240 S31600	65	489	2
INNER SHELL LID LIFTING FEATURE	SA-240 S31600	27	12	1
OUTER SHELL	SB-575 N06022	20	3268	1
EXTENDED OUTER SHELL LID	SB-575 N06022	25	103	1
EXTENDED OUTER SHELL LID BASE	SB-575 N06022	25	221	1
OUTER SHELL LID LIFTING FEATURE	SB-575 N06022	27	13	2
EXTENDED LID REINFORCEMENT RING	SB-575 N06022	50	75	1
OUTER SHELL FLAT CLOSURE LID	SB-575 N06022	10	98	1
OUTER SHELL FLAT BOTTOM LID	SB-575 N06022	25	245	1
UPPER TRUNNION COLLAR SLEEVE	SB-575 N06022	40	404	1
LOWER TRUNNION COLLAR SLEEVE	SB-575 N06022	40	396	1
INNER SHELL SUPPORT RING	SB-575 N06022	20	32	1
TOTAL ALLOY 22 WELDS	SFA-5.14 N06022	-	194	**
TOTAL 316 WELDS	SFA-5.9 S31680	-	59	**
WASTE PACKAGE ASSEMBLY	-	-	19437	1
BWR FUEL ASSEMBLY	-	-	*328.4	24
WASTE PACKAGE ASSEMBLY WITH SNF	-	-	27318	1

* CRWMS M&O 1997. WATE CONTAINER CAVITY SIZE DETERMINATION. BBAA00000-01717-0200-00026 REV 00 LAS VEGAS, NV: CRWMS M&O. ACC: MOL.19980106.0061

** REFER TO SK-0202 REV 00 "24-BWR WASTE PACKAGE ASSEMBLY WELD CONFIGURATION"

SK-0184 REV 00	SHEET 2 OF 2

ATTACHMENT III

Figures obtained from LS-DYNA V950.C for the Tip-over of the 12-PWR Waste Package

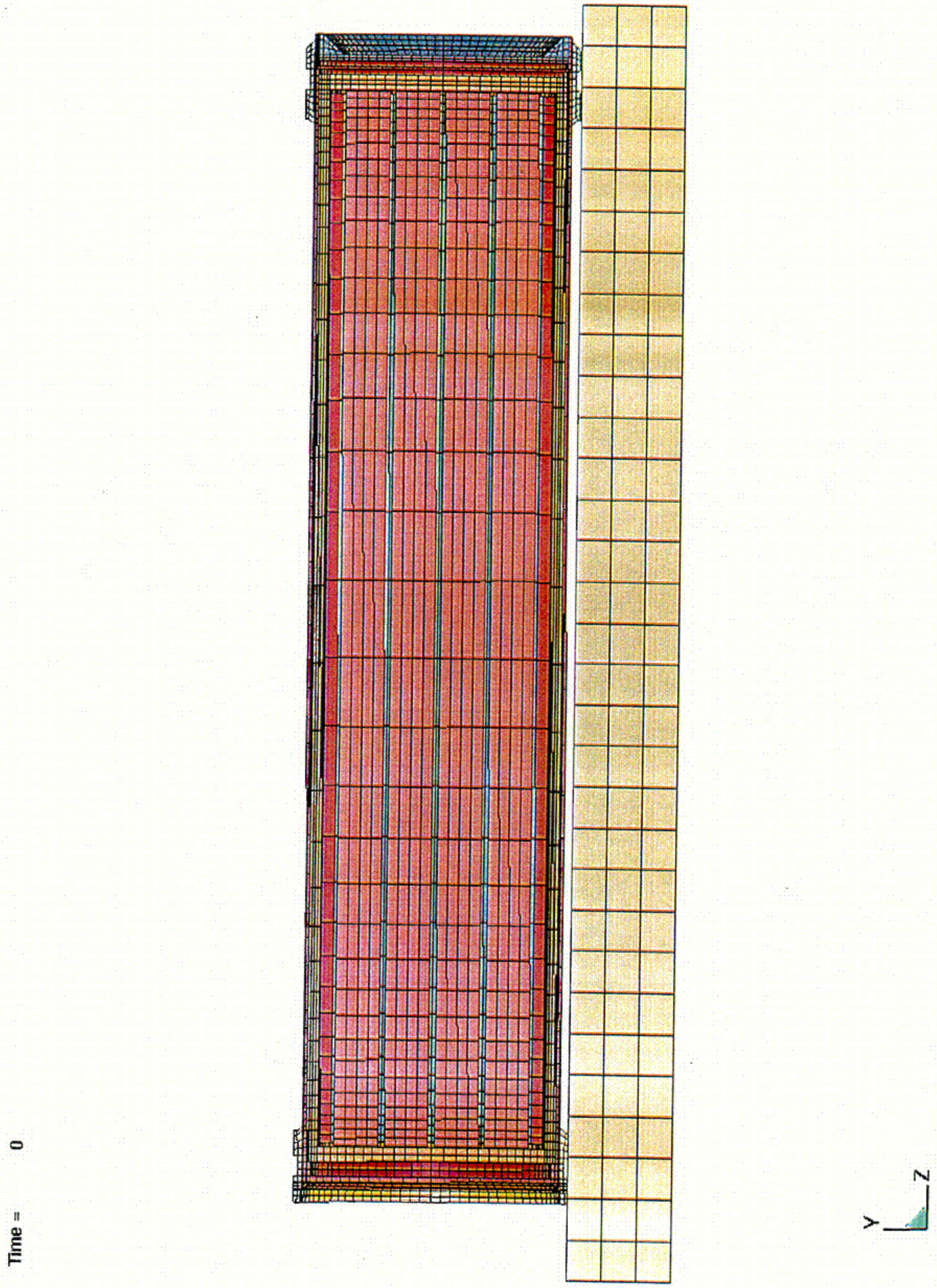

Figure 1: Mesh of the 12-PWR Waste Package

C01

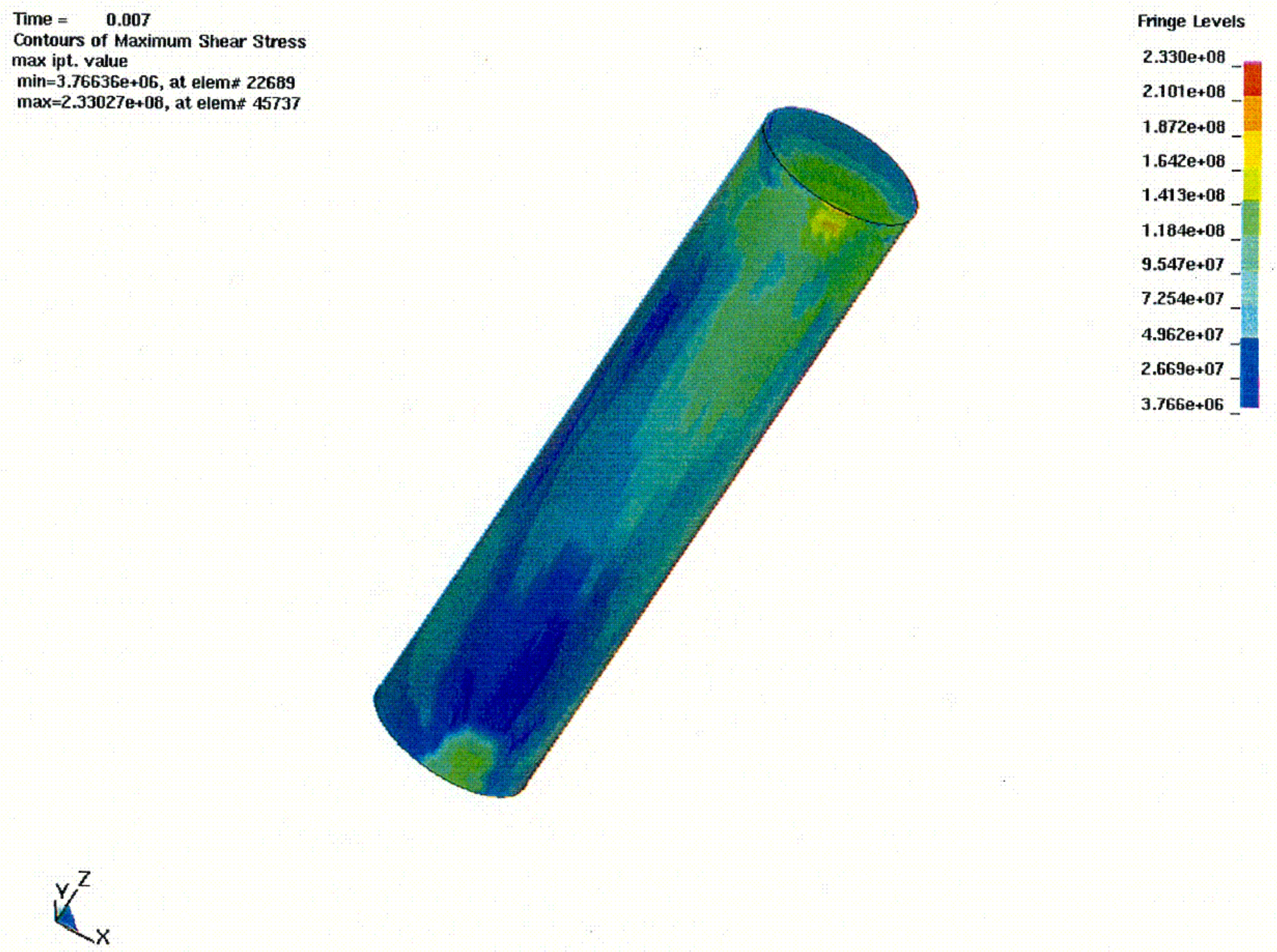

Figure 2: Shear Stress in the 12-PWR Waste Package Inner Shell at RT

C02

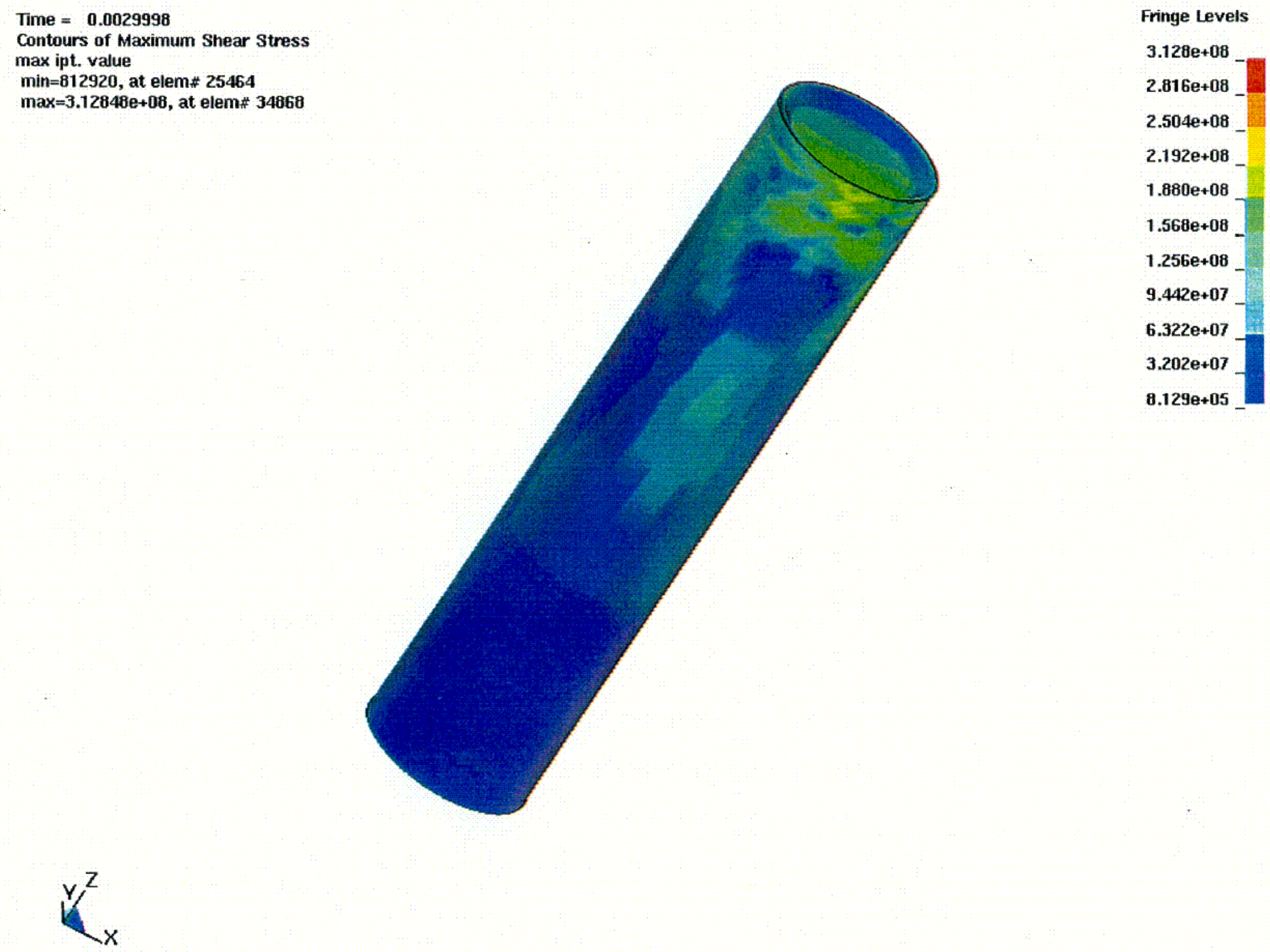

Figure 3: Shear Stress in the 12-PWR Waste Package Outer Shell at RT

C03

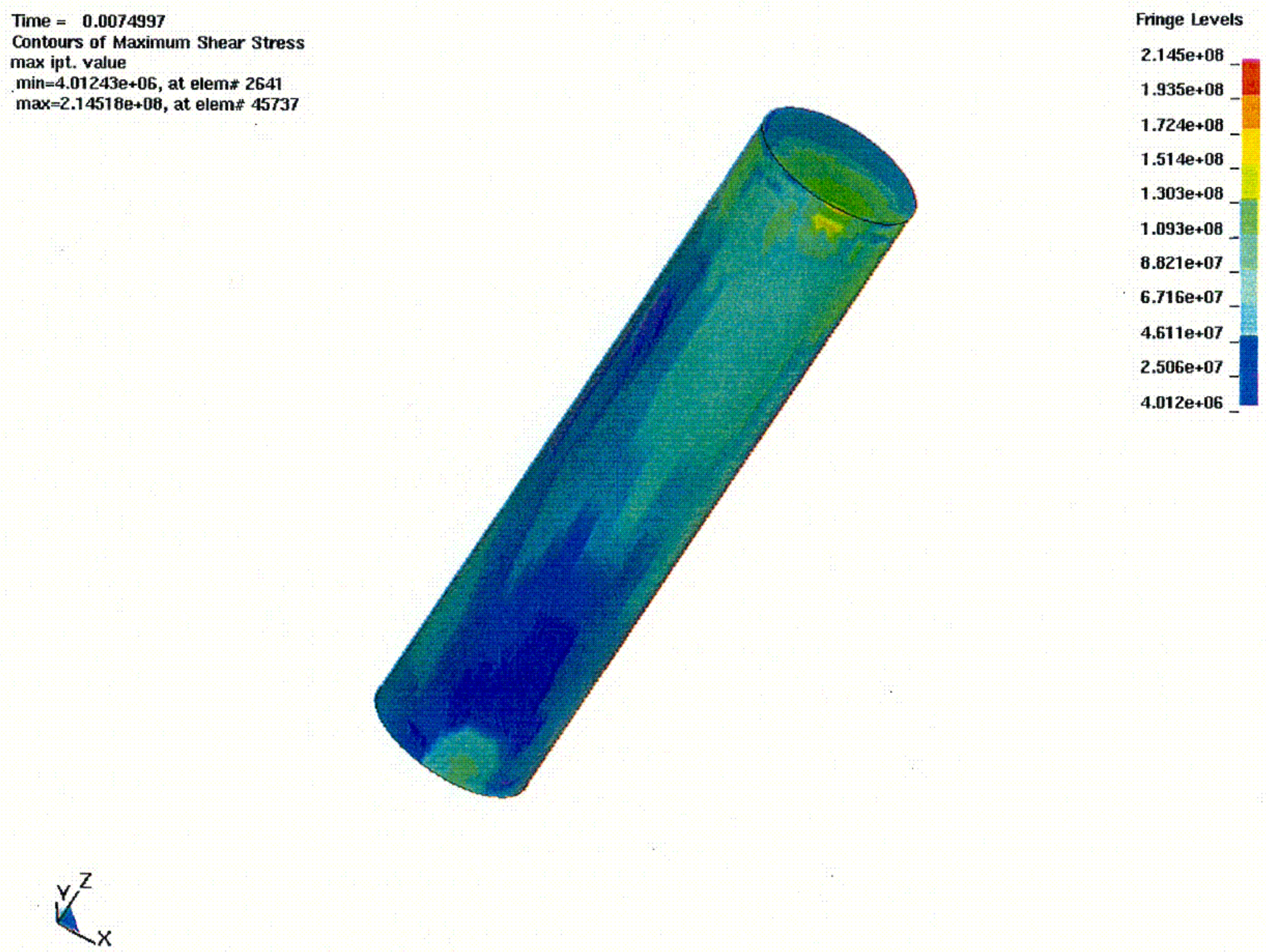

Figure 4: Shear Stress in the 12-PWR Waste Package Inner Shell at 204°C

C04

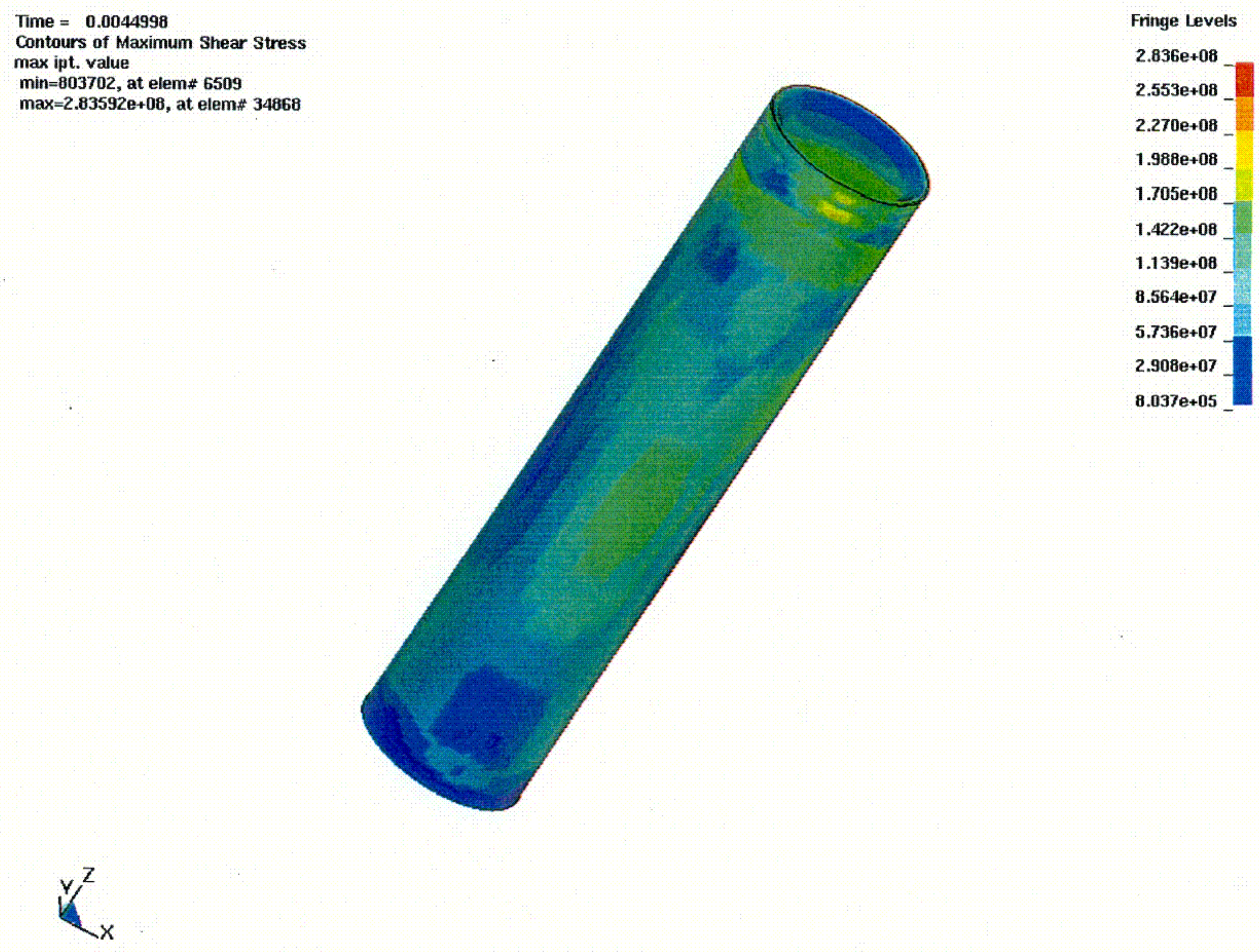

Figure 5: Shear Stress in the 12-PWR Waste Package Outer Shell at 204°C

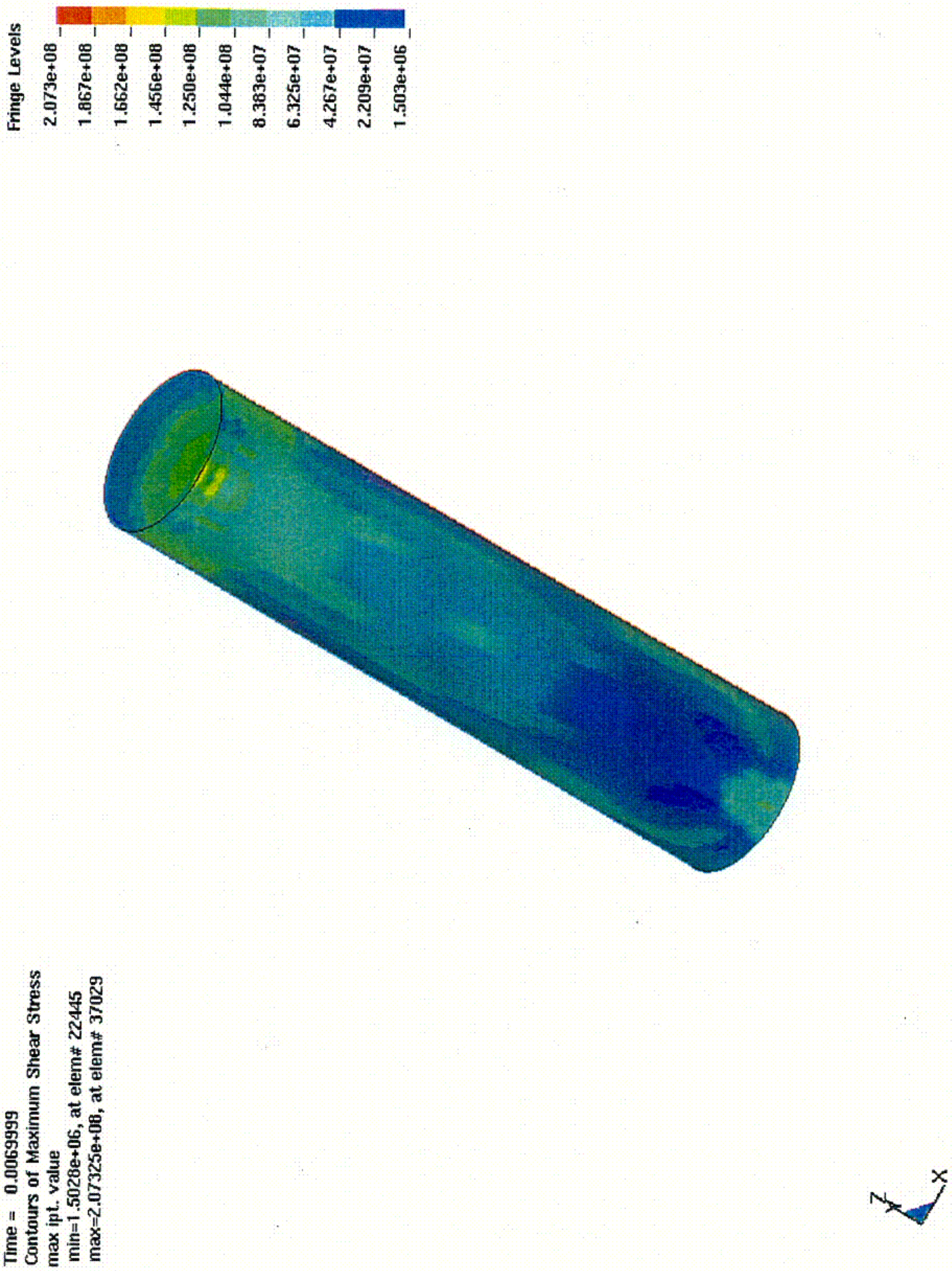

Figure 6: Shear Stress in the 12-PWR Waste Package Inner Shell at 316°C

C06

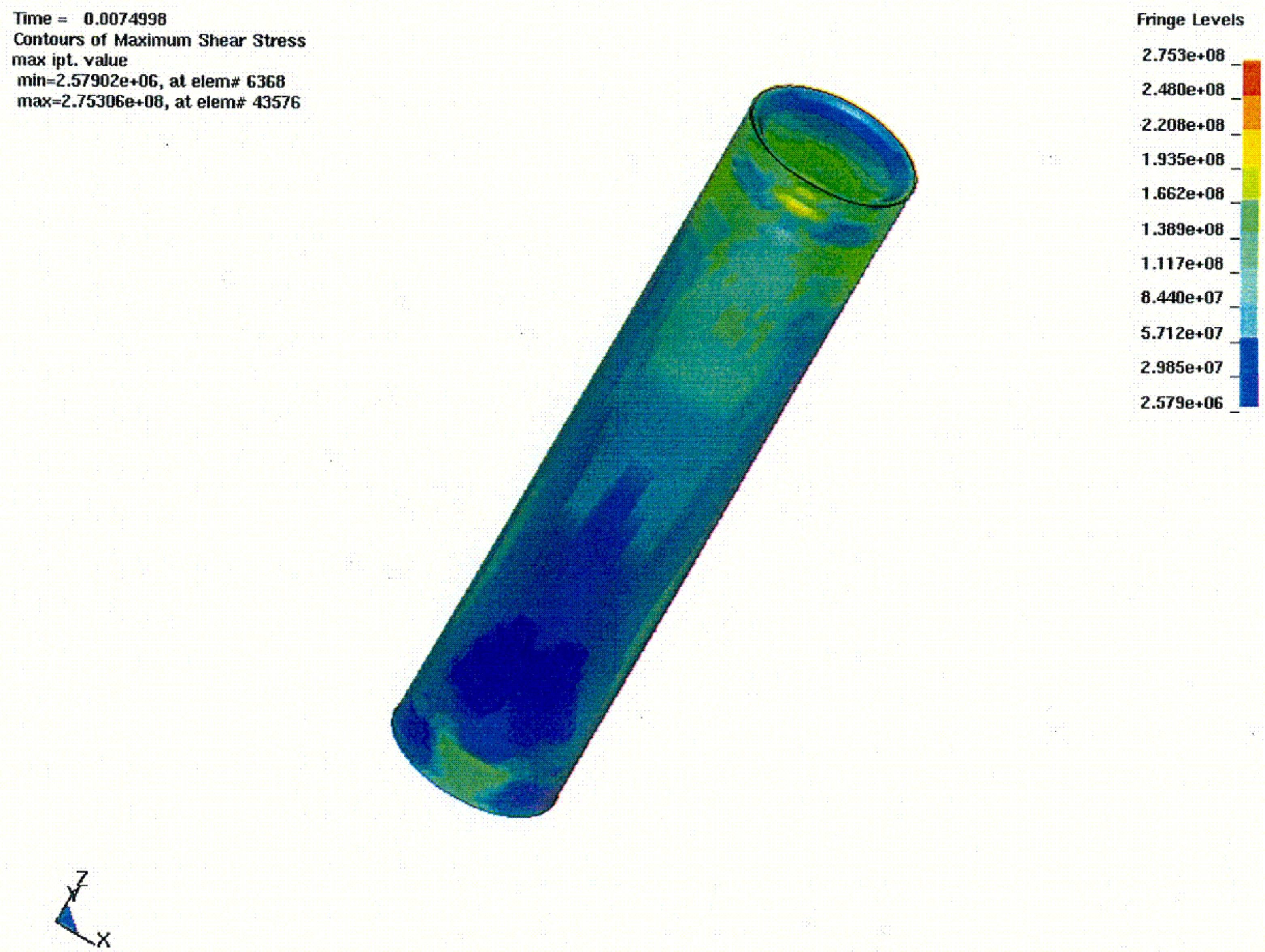

Figure 7: Shear Stress in the 12-PWR Waste Package Outer Shell at 316°C

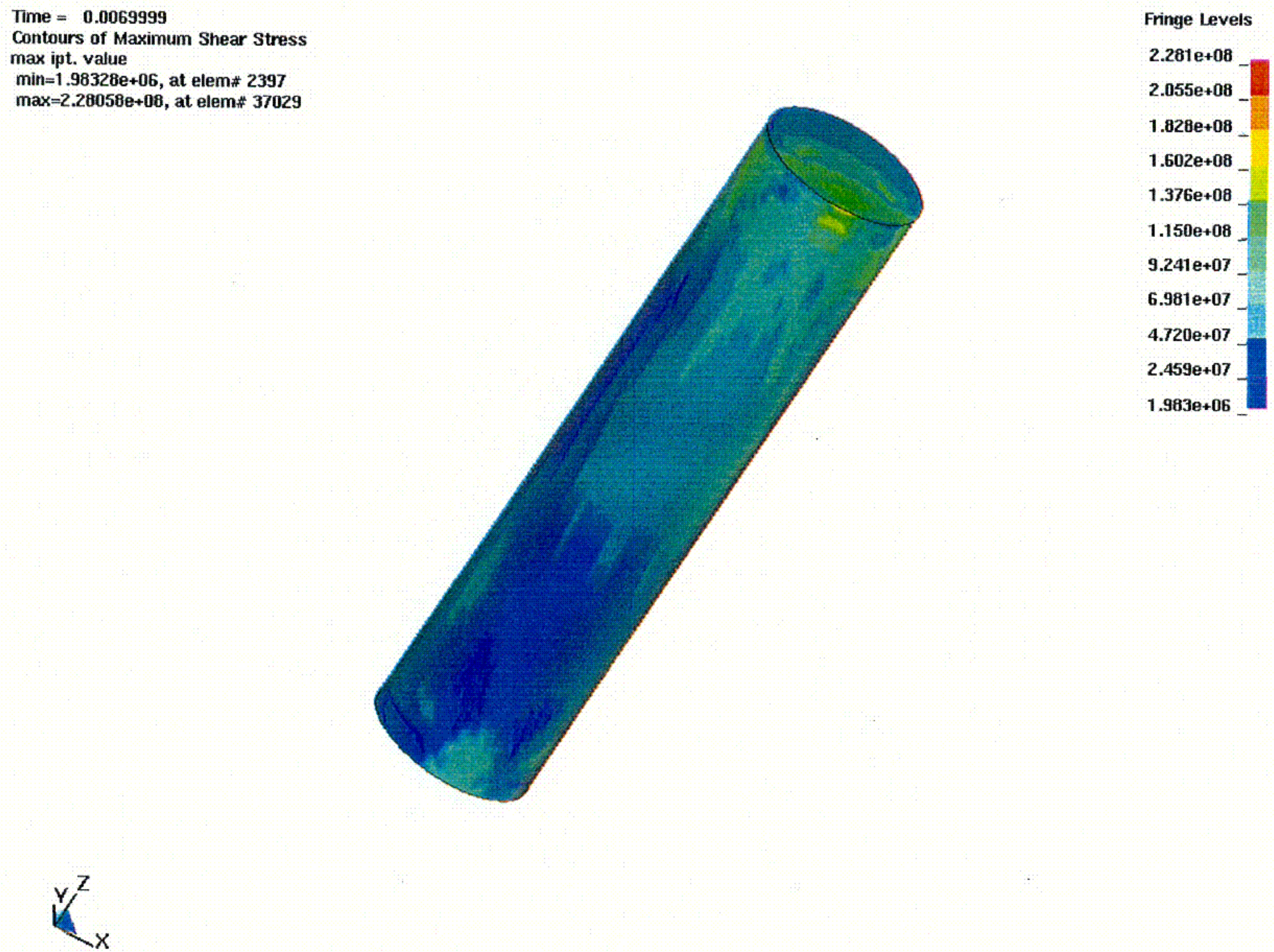

Figure 8: Shear Stress in the 12-PWR Waste Package Inner Shell at 316°*C*, with Modified Elongation

C08

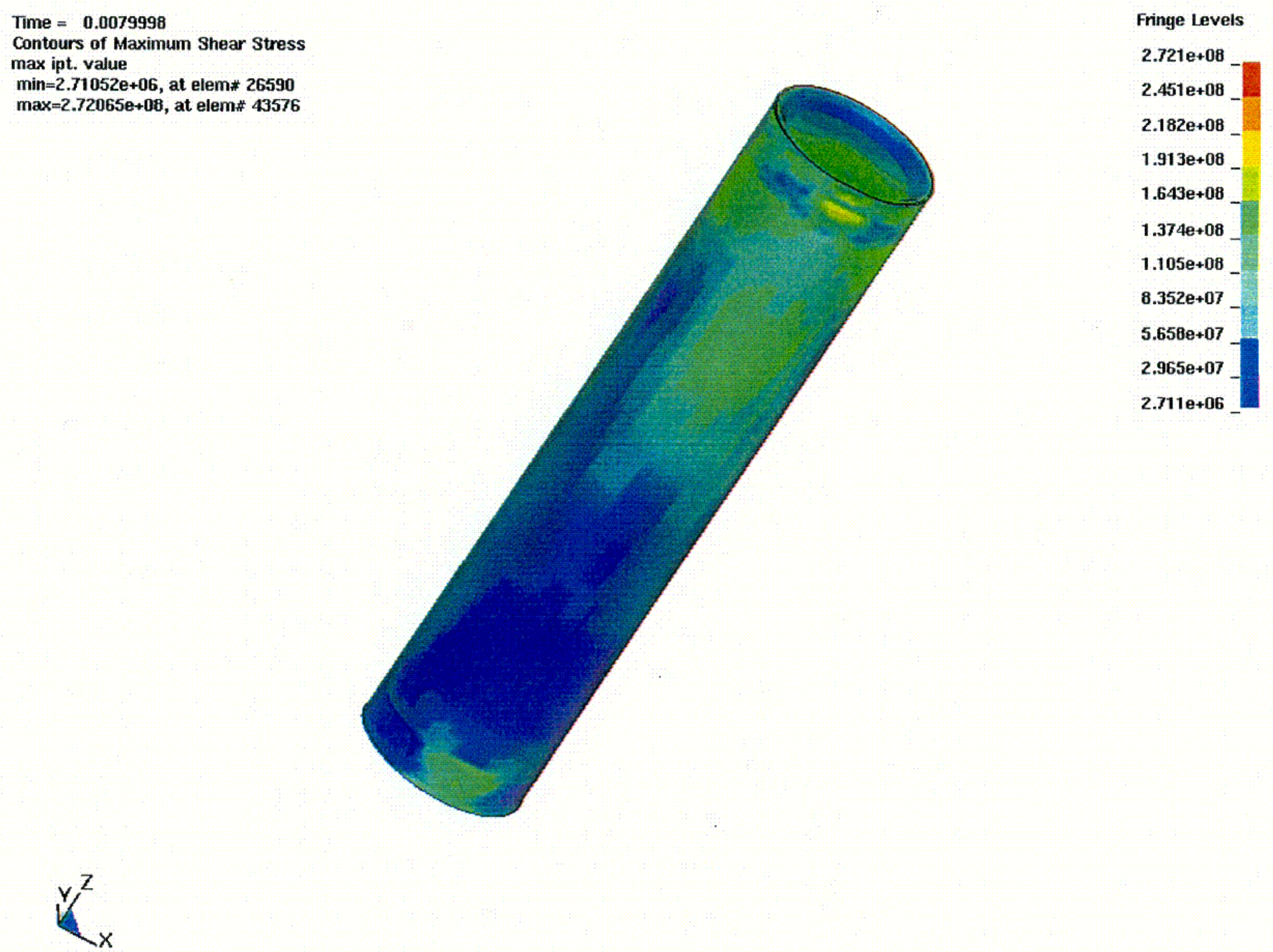

Figure 9: Shear Stress in the 12-PWR Waste Package Outer Shell at 316°C, with Modified Elongation

ATTACHMENT IV

Figures obtained from LS-DYNA V950.C for the Tip-over of the 24-BWR Waste Package

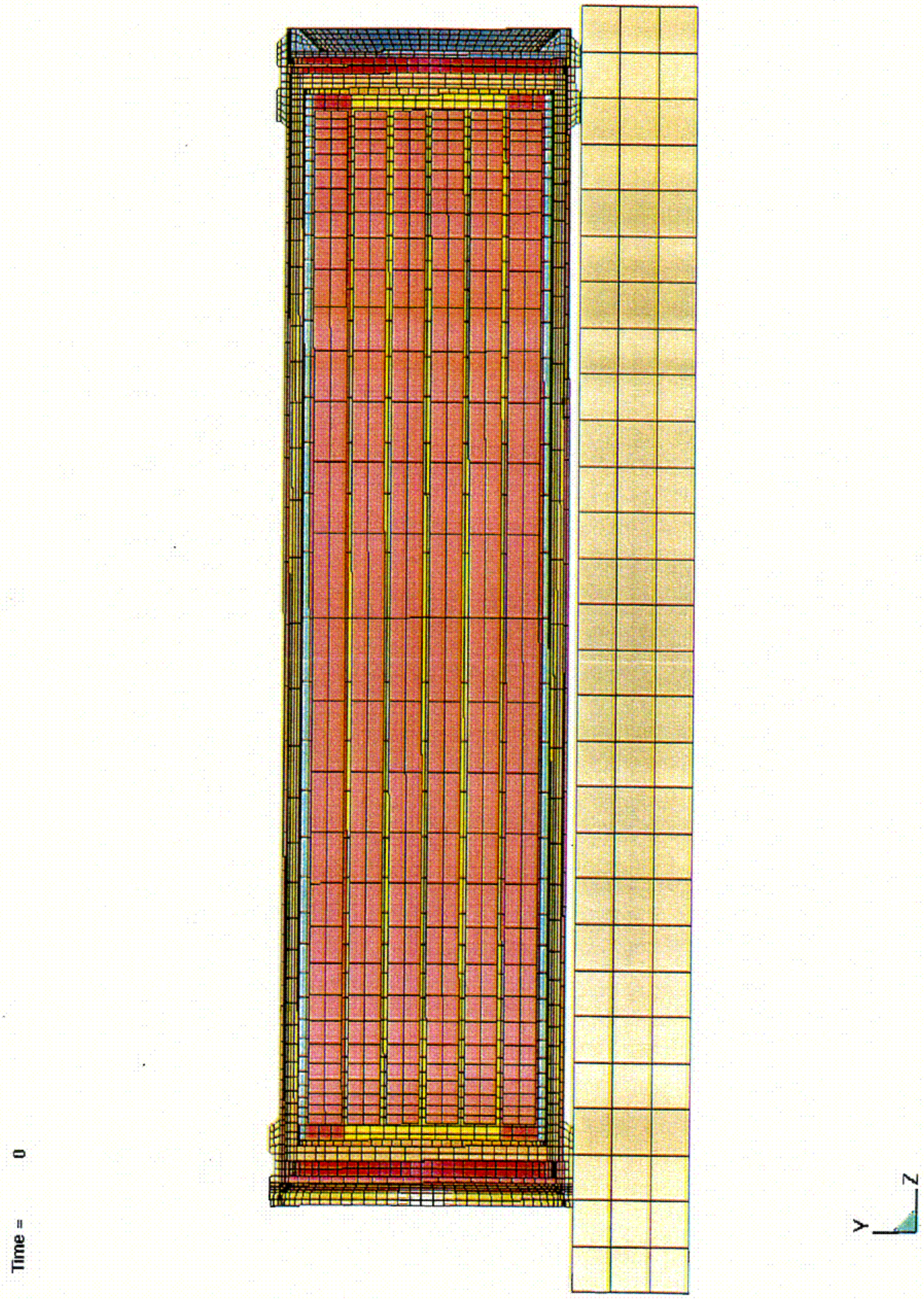

Figure 1: Mesh of the 24-BWR Waste Package

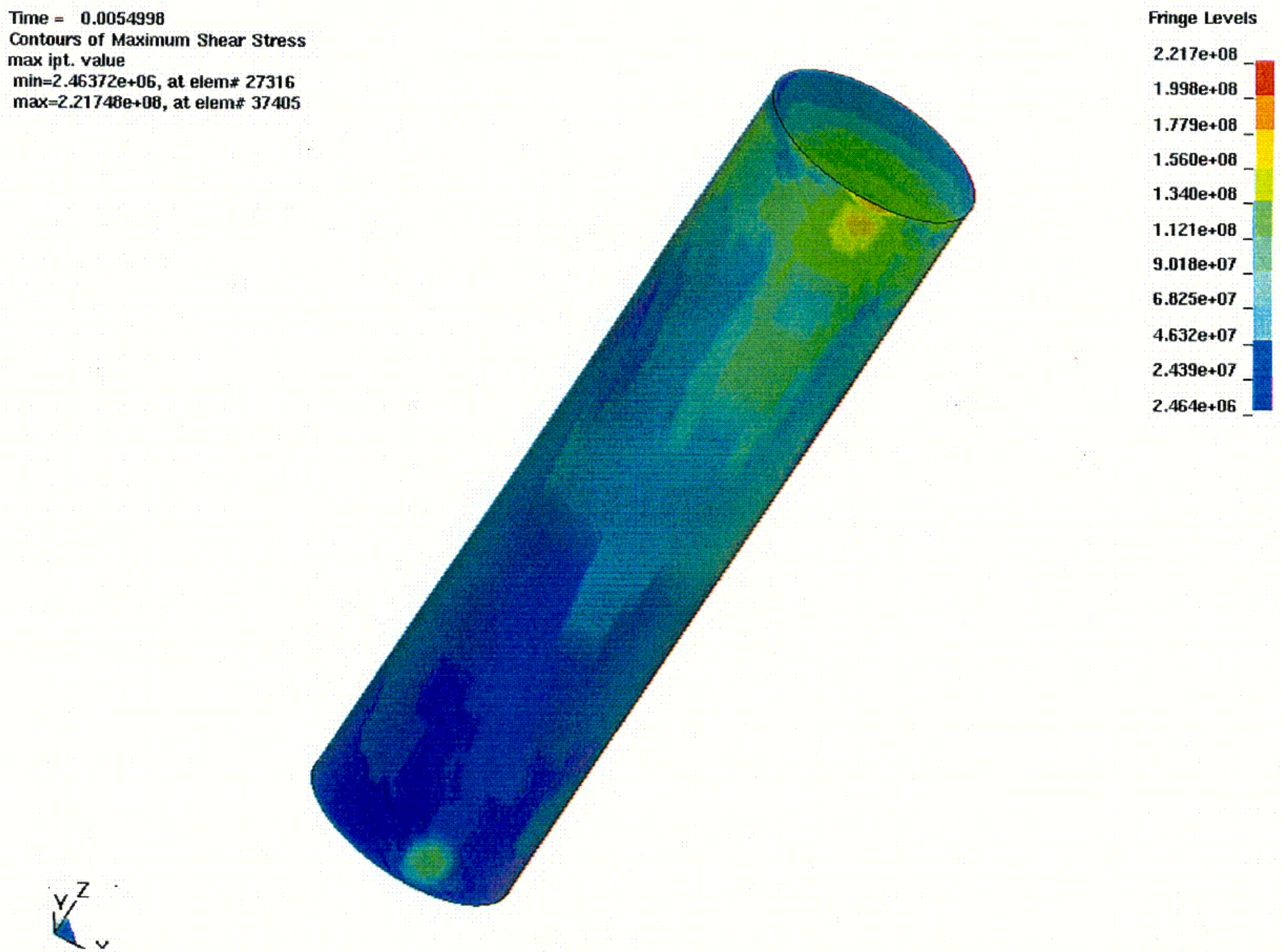

Figure 2: Shear Stress in the 24-BWR Waste Package Inner Shell at RT

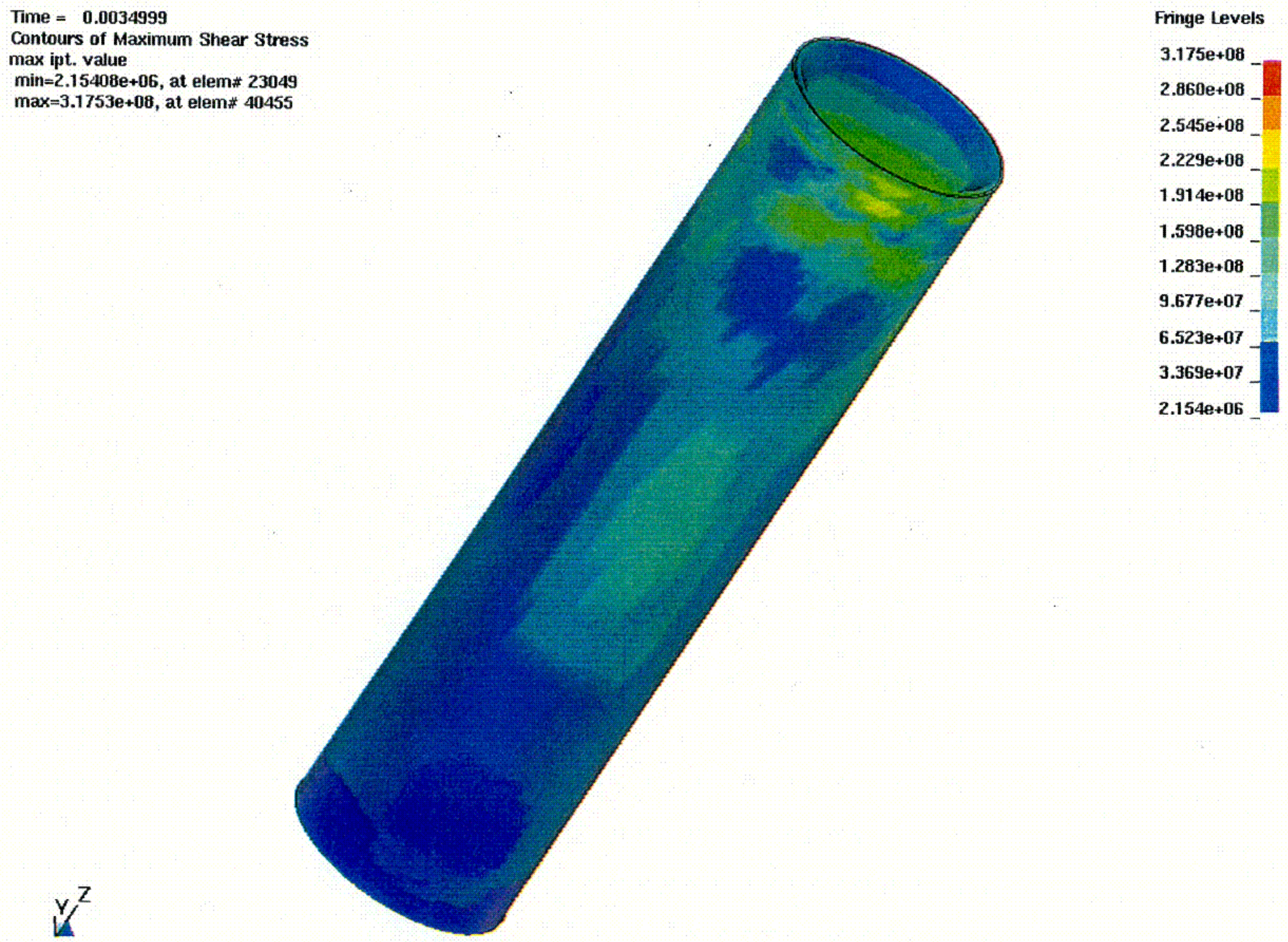

Figure 3: Shear Stress in the 24-BWR Waste Package Outer Shell at RT

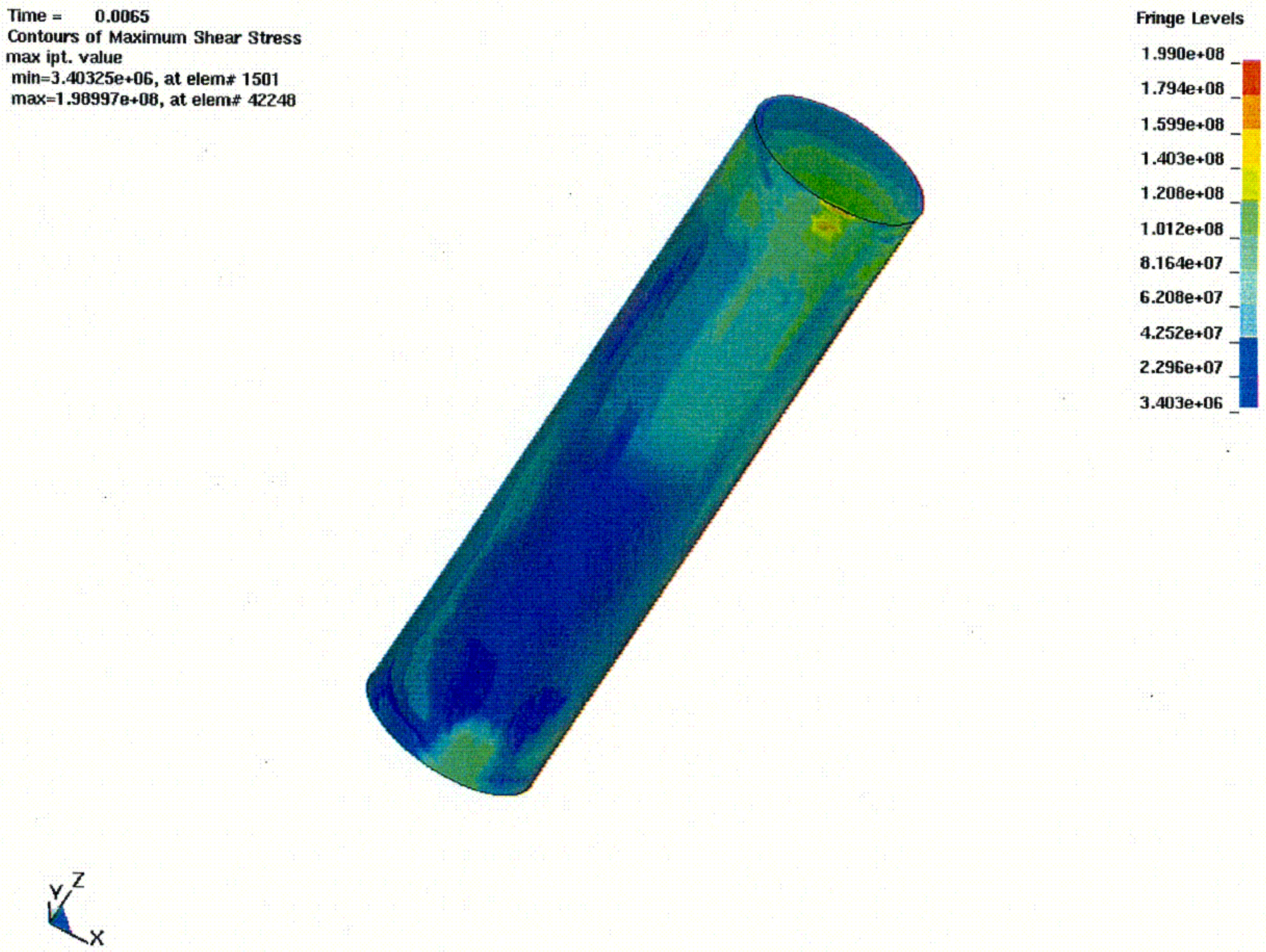

Figure 4: Shear Stress in the 24-BWR Waste Package Inner Shell at 204°C

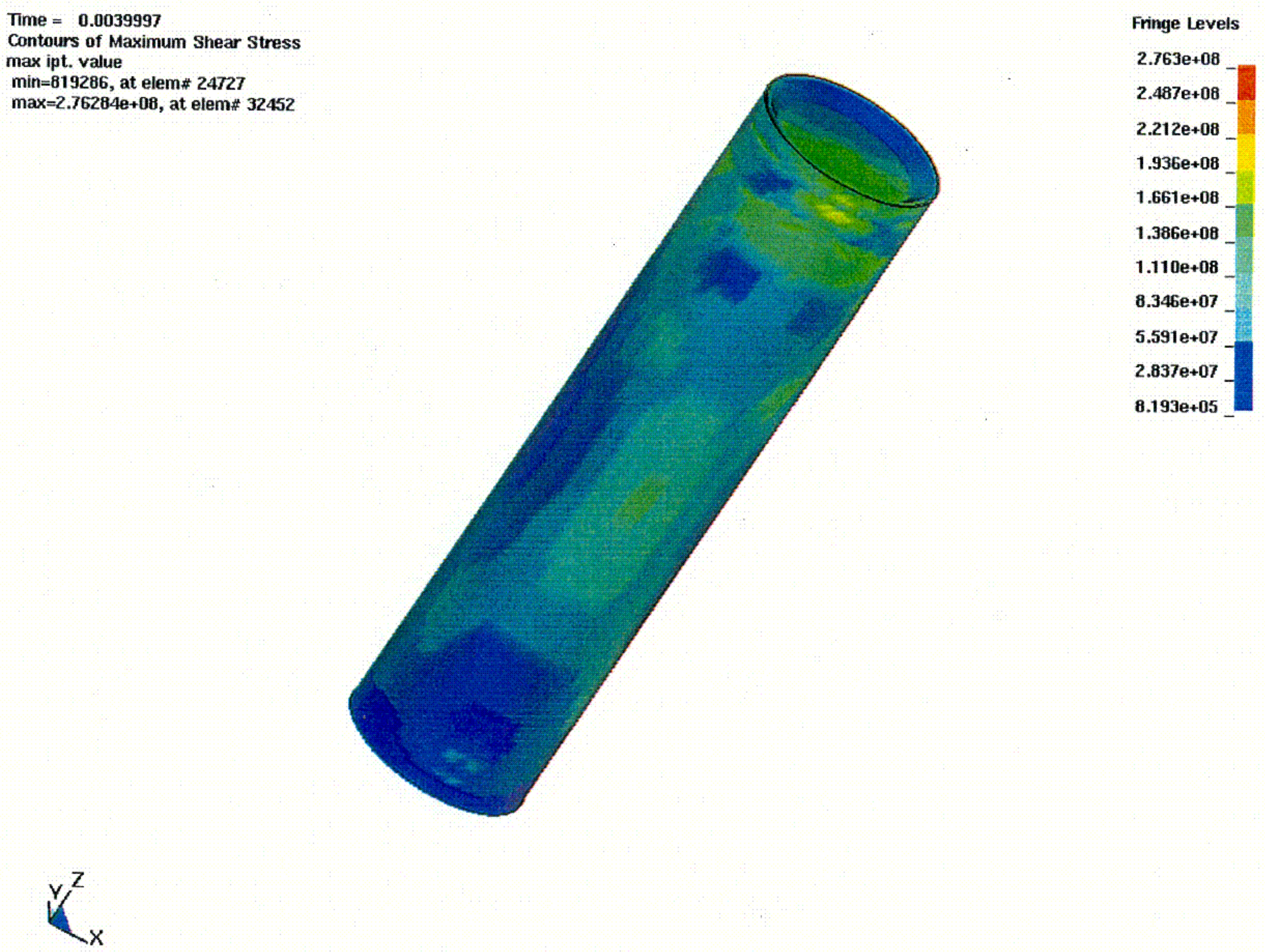

Figure 5: Shear Stress in the 24-BWR Waste Package Outer Shell at 204°C

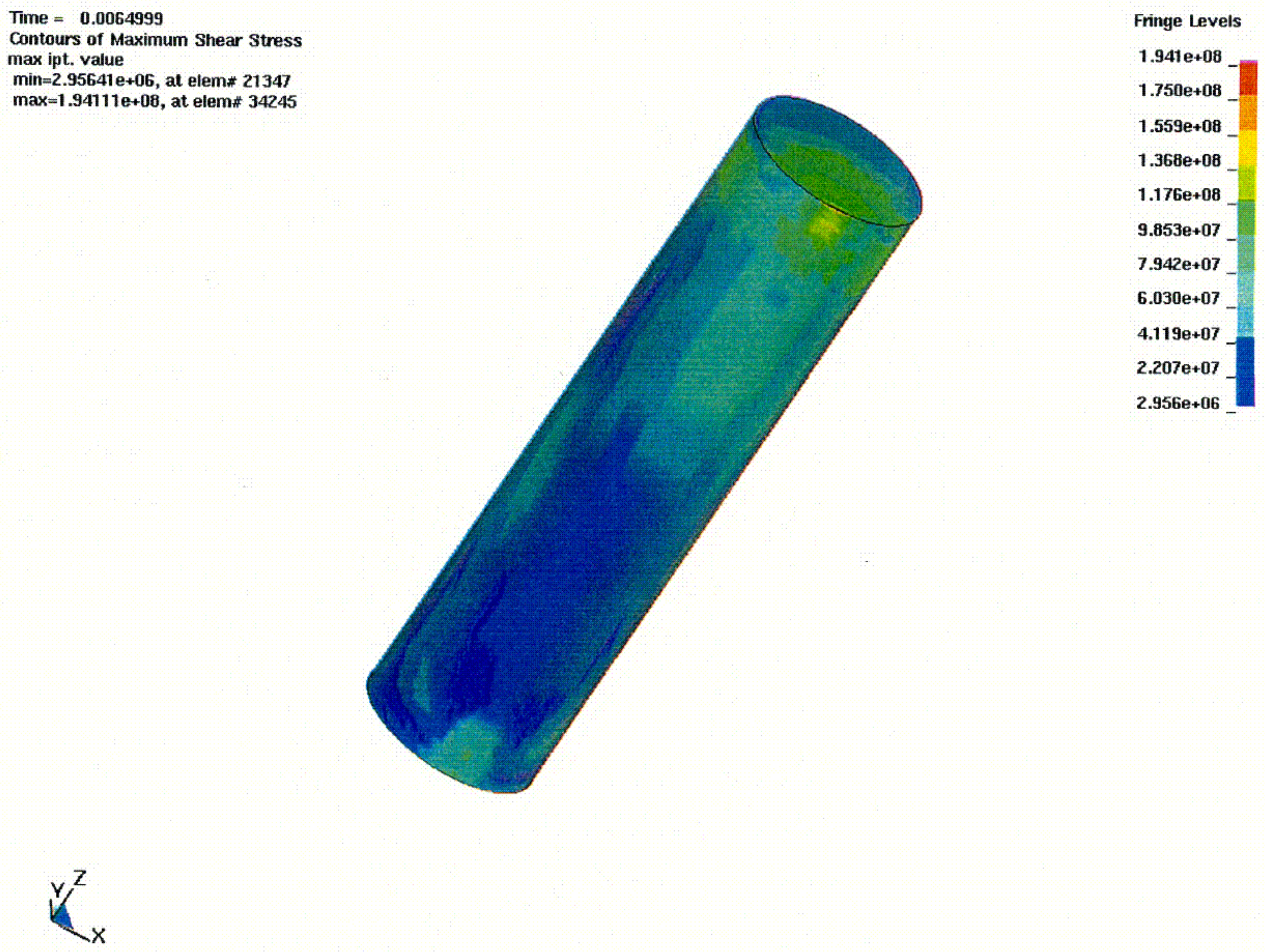

Figure 6: Shear Stress in the 24-BWR Waste Package Inner Shell at 316°C

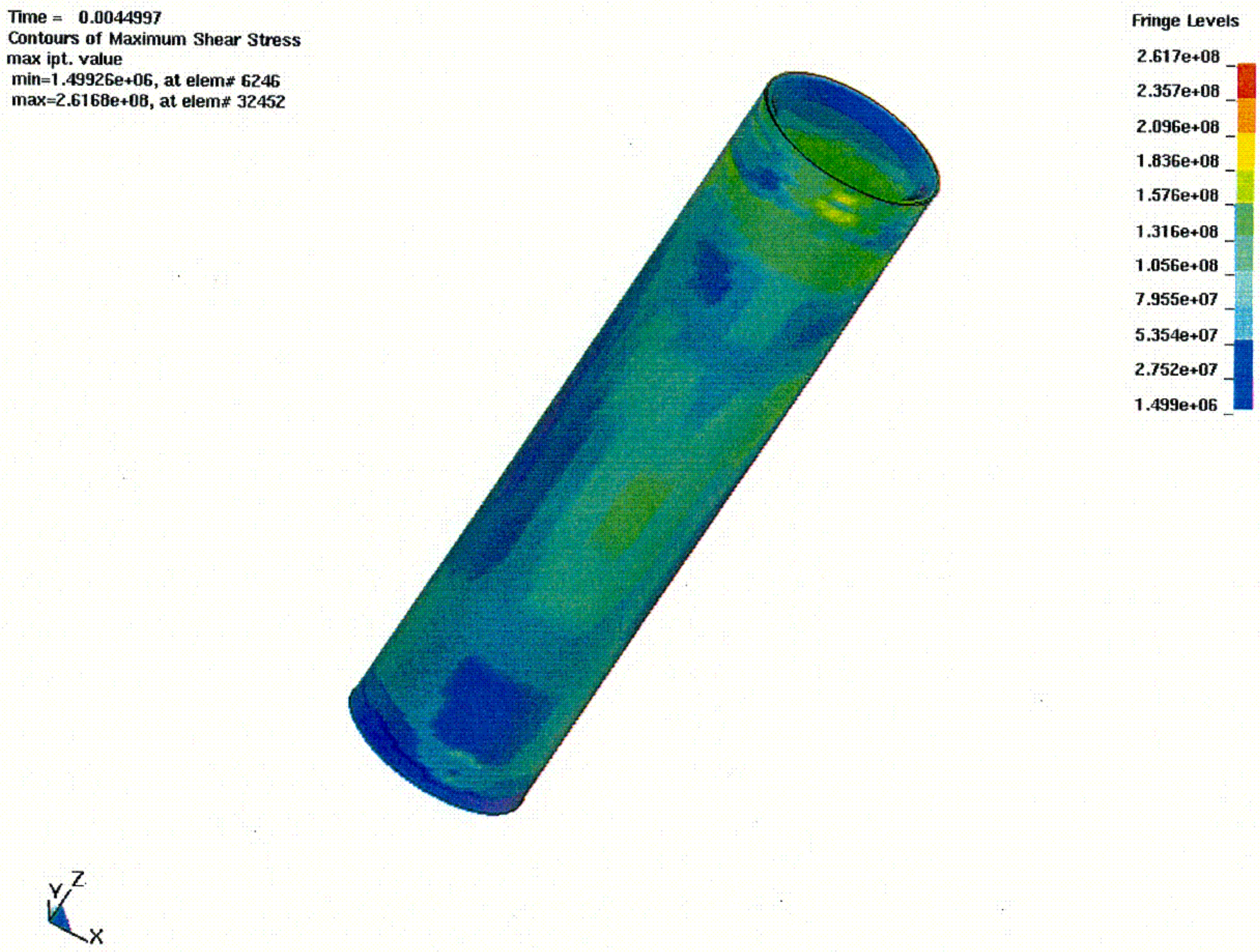

Figure 7: Shear Stress in the 24-BWR Waste Package Outer Shell at 316°C

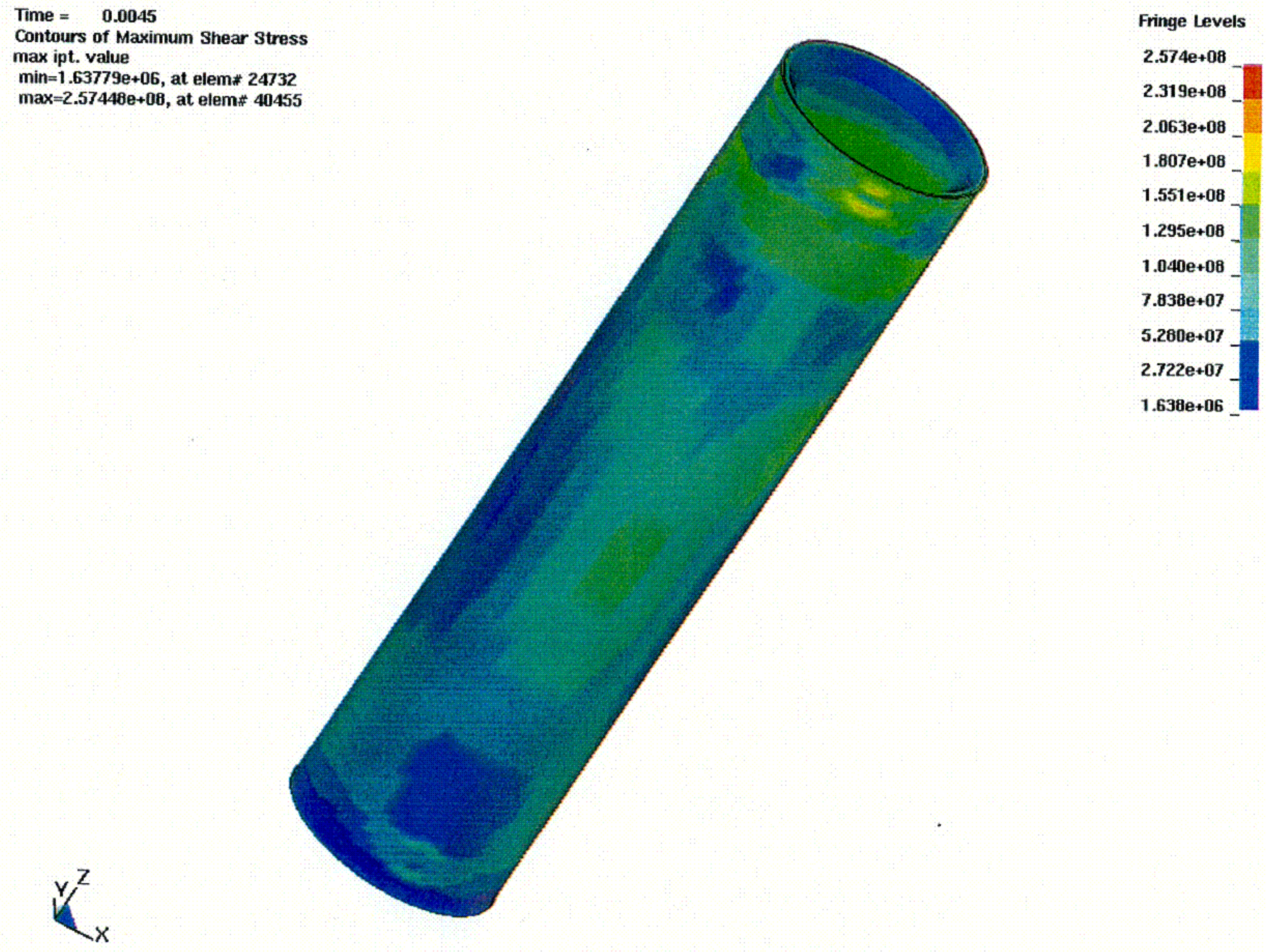

Figure 9: Shear Stress in the 24-BWR Waste Package Outer Shell at 316°C, with Modified Elongation

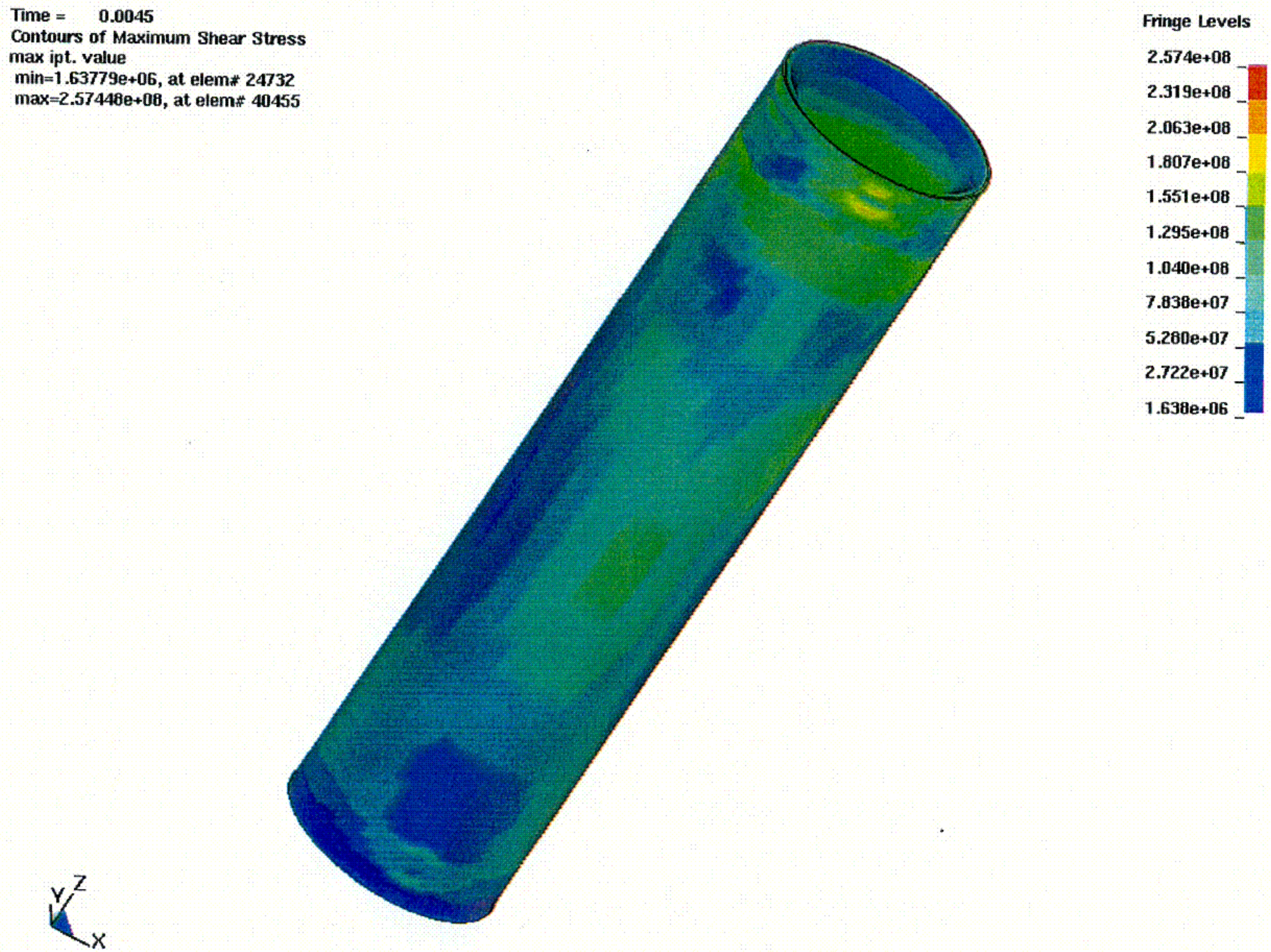

Figure 9: Shear Stress in the 24-BWR Waste Package Outer Shell at 316°C, with Modified Elongation